Online Research @ Cardiff

Citation for final published version:

information services
gwasanaethau gwybodaeth

Dissociable effects of complement C3 and C3aR on survival and morphology of adult born hippocampal neurons, pattern separation, and cognitive flexibility in male mice.

Laura J. Westacott[1,4], Niels Haan[1,4], Claudia Evison[7], Omar Marei[1], Jeremy Hall[1,4],

Timothy R. Hughes[3], Malik Zaben[1,5], B. Paul Morgan[3,4,6], Trevor Humby[1,2,4],

Lawrence S. Wilkinson[1,2,4*] & William P. Gray[1,4,5*†]

Author Affiliations

[1] Neuroscience and Mental Health Research Institute, MRC Centre for Neuropsychiatric Genetic and Genomics, School of Medicine, Hadyn Ellis Building, Cardiff University, Cardiff, CF24 4HQ, UK.
[2] Behavioural Genetics Group, Schools of Psychology and Medicine, Cardiff University, Cardiff, CF10 3AT, UK.
[3] Complement Biology Group, Systems Immunity Research Institute, School of Medicine, Cardiff University, CF14 4XW, Cardiff UK.
[4] Hodge Centre for Neuropsychiatric Immunology, School of Medicine, Cardiff University, Cardiff CF24 4HQ, UK.
[5] Brain Repair and Intracranial Neurotherapeutics (BRAIN), Biomedical Research Unit, Division of Psychological Medicine and Clinical Neurosciences, School of Medicine, Cardiff University, CF24 4HQ, UK.
[6] UK Dementia Research Institute, Cardiff University, Cardiff, CF24 4HQ, UK.
[7] National Centre for Mental Health, Hadyn Ellis Building, Cardiff University, Cardiff, CF24 4HQ, UK.

*Joint senior authors

†**Corresponding Author:** Prof William Gray
Email: GrayWP@cardiff.ac.uk
Address: Brain Repair and Intracranial Neurotherapeutics (BRAIN), Biomedical Research Unit, Division of Psychological Medicine and Clinical Neurosciences, School of Medicine, Cardiff University, CF24 4HQ, UK.

Key words: Complement system, adult neurogenesis, morphology, hippocampus, pattern separation, cognitive flexibility

Abbreviations: AHN; adult hippocampal neurogenesis, C3; complement component 3, C3aR; complement C3a receptor, GCs; granule cells, GCL; granule cell layer.

Abstract

Adult hippocampal neurogenesis (AHN) is a form of ongoing plasticity in the brain that supports specific aspects of cognition. Disruptions in AHN have been observed in neuropsychiatric conditions presenting with inflammatory components and are associated with impairments in cognition and mood. Recent evidence highlights important roles of the complement system in synaptic plasticity and neurogenesis during neurodevelopment and in acute learning and memory processes. In this work we investigated the impact of the complement C3/C3aR pathway on AHN and its functional implications for AHN-related behaviours. In $C3^{-/-}$ mice, we found increased numbers and accelerated migration of adult born granule cells, indicating that absence of C3 leads to abnormal survival and distribution of adult born neurons. Loss of either C3 or C3aR affected the morphology of immature neurons, reducing morphological complexity, though these effects were more pronounced in the absence of C3aR. We assessed functional impacts of the cellular phenotypes in an operant spatial discrimination task that assayed AHN sensitive behaviours. Again, we observed differences in the effects of manipulating C3 or C3aR, in that whilst $C3aR^{-/-}$ mice showed evidence of enhanced pattern separation abilities, $C3^{-/-}$ mice instead demonstrated impaired behavioural flexibility. Our findings show that C3 and C3aR manipulation have distinct effects on AHN that impact at different stages in the development and maturation of newly born neurons, and that the dissociable cellular phenotypes are associated with specific alterations in AHN-related behaviours.

75

1. Introduction

77 Adult hippocampal neurogenesis (AHN) is a unique process that recapitulates the

78 steps of developmental neurogenesis in an otherwise anti-neurogenic brain, from

79 precursor proliferation, fate specification, migration and differentiation to morphological

80 and synaptic integration of newly born neurons[1]. Originating from radial glial cells,

81 neuronal progenitor cells are born in their thousands within the sub granular zone of

82 dentate gyrus[2]. While the majority of these cells undergo programmed cell death within

83 the first few weeks of life[3], surviving immature granule cell (GC) neurons progress

84 through a multifaceted developmental process as they mature and integrate into the

85 hippocampal circuitry[4].

86 The function of AHN has been debated but current evidence suggests it is involved

87 in information processing critical to adaptive behaviour across a number of areas

88 including learning, memory and emotionality[5-7]. In particular, young adult born neurons

89 are thought to perform pattern separation, the process that enables discrimination of

90 highly similar, overlapping spatial and temporal stimuli, fostering the appropriate

91 separation and storage of similar memory traces or engrams thereby reducing

92 interference[8,9]. Key evidence supporting a role for AHN in pattern separation comes

93 from studies in which ablation of neurogenesis resulted in specific impairments in

94 discriminating stimuli with a high degree of spatial similarity or overlap, but not stimuli

95 that are more readily distinguished[10-12]. Evidence also supports an important role for

96 AHN in cognitive flexibility and the underlying processes of behavioural inhibition that

97 allows flexible responding in the face of changing contingencies[5], and elements of

98 cognitive flexibility and behavioural inhibition have been shown to be sensitive to

99 experimental manipulations of AHN[13-17].

The process of AHN is subject to regulation by myriad factors, including microglia and immune signalling[18,19]. The complement system consists of separate activation pathways which converge on a single molecule, C3, and then culminate in the terminal pathway[20]. It is through C3 activation that the main effectors of the complement system are generated, including the anaphylatoxin C3a. This peptide signals via its cognate G protein-coupled C3a receptor (C3aR) to stimulate intracellular signalling pathways leading to the modulation of critical cellular functions[21] and pro- and anti-inflammatory actions[22]. In recent years, prominent roles have emerged for the complement system in brain development, including synapse elimination[23] and embryonic neurogenesis[24], but also in neurodegeneration[25-27] though how complement may influence ongoing neurogenesis and cognitive functions within the adult brain have received relatively little focus. Given converging evidence of aberrant adult neurogenesis[28,29] and cognitive dysfunction[30-32] in neuropsychiatric disorders associated with abnormal complement activity[33,34], it is important that we improve our understanding of how complement may regulate ongoing neuroplasticity and neurodevelopment in the context of AHN.

Previous literature illustrates conflicting roles for different complement pathways in regulating basal AHN. Adult *C3*$^{-/-}$ and *C3aR*$^{-/-}$ mice, and wildtype mice in which C3aR was pharmacologically blocked, showed reduced numbers of adult born neurons[35], suggesting that the C3a-C3aR axis is a positive regulator of AHN. In contrast, another report focusing on the role of a different breakdown product of C3, found an inhibitory role of C3d/CR2 signalling in adult neurogenesis, whereby *CR2*$^{-/-}$ mice showed elevated levels of basal neurogenesis in the adult hippocampus[36]. Therefore, two opposing regulatory roles have been assigned to these separate breakdown products of C3, which suggest both pro and anti-neurogenic properties of the complement

system under physiological conditions. Furthermore, the functional consequences of these changes for cognition are unknown. Improved spatial memory recall and reversal learning have been described in *C3*^{-/-} mice[37,38], and blockade of the C3a receptor improved cognition in pathological contexts[26,27,39], but there have not yet been any direct investigations of AHN-associated cognition in complement knockout models.

Other important variables in the neurogenic process include the morphology and functional integration of newborn neurons into the existing hippocampal circuitry[40]. In addition to the aforementioned roles of complement in sculpting neuronal circuitry in the developing brain[23,41], several studies have implicated the C3a/C3aR axis in modulating neuronal morphology *in vitro*[39,42,43]. Whether complement is involved in the morphological maturation of adult born neurons *in vivo* within the hippocampal neurogenic niche has not yet been reported.

Using mice constitutively deficient in complement *C3* or *C3aR,* we investigated the impact of these pathways on discrete stages of the neurogenic process occurring in the adult hippocampus. We also assessed behaviour in a translational touch-screen visual discrimination task previously employed to demonstrate the involvement of AHN in pattern separation[10,12,44]. Our findings reveal different effects of C3 and C3aR manipulation on AHN and related behaviours. Cellular effects of C3aR deficiency were mainly limited to effects on the morphological complexity of adult born neurons, whilst C3 deficiency impacted predominantly on their survival and ultimate location. The dissociations in cellular effects were associated with different behavioural outcomes and together the data suggest cellular mechanisms linking C3aR to pattern separation and C3 to cognitive flexibility, respectively.

2. Materials and Methods

For full methods, see *Supplementary Information.*

2.1 Mouse models and husbandry

Wildtype and $C3^{-/-}$ strains were sourced in-house from Professor B. Paul Morgan and Dr Timothy Hughes (strains originally from The Jackson Laboratory; B6.PL-Thy1^{a}/CyJ stock#000406 and B6;129S4-C3tm1Crr/J stock#003641 respectively). $C3aR^{-/-}$ mice were provided by Professor Craig Gerard of Boston Children's Hospital, USA (mice subsequently provided to The Jackson Laboratory by Prof. Gerard, strain B6.129S4(C)-$C3ar1^{tm1Cge}$/BaoluJ). $C3^{-/-}$ and $C3aR^{-/-}$ mice were maintained via homozygous breeding on a C57Bl/6J background and in all experiments were compared to wildtype mice also on a C57Bl/6J background. Male mice were kept in a temperature and humidity-controlled vivarium (21±2°C and 50±10%, respectively) with a 12-hour light-dark cycle (lights on at 07:00hrs/lights off at 19:00hrs). For ex vivo histological analyses, animals were between 8 and 12 weeks of age at the time of sacrifice. For behavioural testing, animals were habituated to daily handling by the experimenter for 2 weeks prior to beginning behavioral testing at 8 weeks of age and were approximately 22 weeks of age on completion. All procedures were performed in accordance with the requirements of the UK Animals (Scientific Procedures) Act (1986).

2.2 Pulse-chase experiments

Animals were injected with 5-bromo-2'-deoxyuridine (Sigma Aldrich, UK) diluted in sterile Phosphate buffered saline (pH 7.4) at a dose of 100 mg/kg i.p either 6 hours

174   prior to sacrifice (short pulse BrdU) or once daily on 5 consecutive days, with sacrifice

175   30 days after the first dose (long pulse BrdU).

176   **2.3 Tissue sampling and Immunohistochemistry**

177   Paraformaldehyde fixed brain tissue was sectioned on a cryostat, with 6 sections

178   collected per animal, spanning the longitudinal axis of the hippocampus beginning

179   approximately -0.94 mm from bregma and ending at approximately -3.40 mm from

180   bregma [45]. Sections were selected using a stereological sampling rate of 1/10. Free

181   floating 40μm sections were used for immunohistochemistry (see Supplementary

182   Information).

183   **2.4 Microscopy**

184   Tissue sections were imaged on an upright Leica DM6000B fluorescence microscope

185   using tile scanning at 40x magnification to capture the entire left and right dentate gyri

186   in each section. Experimenters were blinded to genotype during all analyses.

187   **2.5 Cell counting and analyses**

188   In order to estimate the total number of cells (e.g., DCX^+, $BrdU^+$, $NeuN^+$) in the whole

189   dentate gyri of each animal, the number of cells counted in the left and right dentate

190   were summed and multiplied by the intersection interval (10) to obtain the total number

191   of cells for the region spanning the current section until the next section. This was

192   repeated for each of 6 sections, and the estimates obtained were summed in order to

193   give a measure of the total number of cells present in the entire DG per animal. For

194   migration analyses, the thickness of the GCL was measured in each section and

195   divided into four equally sized bins, each approximately two cells thick and the first of

196   which represented the sub granular zone (SGZ). The distance of individual $BrdU^+$ cells

from the inner (hilar) portion of the SGZ was measured using ImageJ and the total
number and proportions of cells per bin was calculated.

2.6 Sholl analyses

DCX^{+} cells were systematically randomly sampled and traced using Simple neurite
tracer plugin[46] for ImageJ software (https://imagej.net/Fiji). Any cells with processes
not entirely visible were excluded from analyses. For each cell, processes were traced
manually. Primary and secondary path lengths were extracted, before Sholl analysis
was performed. For all experiments detailed, radii separated by a distance of 10 μm
were used. We compared sholl profiles using a single metric, the area under the curve
(AUC). In addition, we analysed the Branching Index (BI), which produces a value that
is proportioned to differences in the pattern of neurite ramification, and is relative to
the amount of branches a neurite possesses[47]. Data on primary path lengths
(processes emanating directly from the soma) and branches (defined as any process
originating from a primary process) was collected in addition to branch numbers.

2.7 Behavioural testing

All behavioural testing was conducted within the light phase. Genotypes were
counterbalanced across morning and afternoon testing sessions. For the duration of
testing, water was restricted to a two-hour access period per day. Body weight was
monitored throughout the period of water deprivation, and animals were maintained at
90% of their free-feeding body weight prior to commencing water restriction. All
subjects had *ad libitum* access to food in the home-cage throughout the behavioural
testing period. All apparatus was cleaned thoroughly in between experimental subjects
using 70% ethanol solution to remove odours.

2.7.1 Locomotor activity (LMA)

LMA was assessed in a 120-minute session conducted in the dark within a plexiglas chamber spanned transversely by two infrared beams.

2.7.2 Habituation to condensed milk

To habituate animals to the reward (condensed milk) to be used in the location discrimination task, animals were given the opportunity to consume either condensed milk or water. Preference for condensed milk was calculated as a percentage of total consumption for each of the five days during which water and milk were available.

2.7.3 Location discrimination task

To assess pattern separation, we used an adaptation of the Location Discrimination (LD) task as described in Hvoslef-Eide et al. (2013)[48] and originally reported by McTighe et al. (2009)[49]. In order to facilitate daily testing of our large behavioural cohort, we implemented shorter, 20 minute test sessions rather than the 60 minute originally reported[10,12,44,50,51]. Within each session, subjects could complete a maximum of 60 trials. The task was delivered in a touch screen operant chamber (Campden Instruments Ltd., UK; Figure 1A). Animals first went through a period of shaping (Figure 1B,i-ii), which accustomed them to making nose-poke responses to illuminated square stimuli at the front of the chamber, for which they received a reward of condensed milk. Having completed shaping, subjects were moved onto task training on a case-by-case basis to prevent overtraining [48].

241
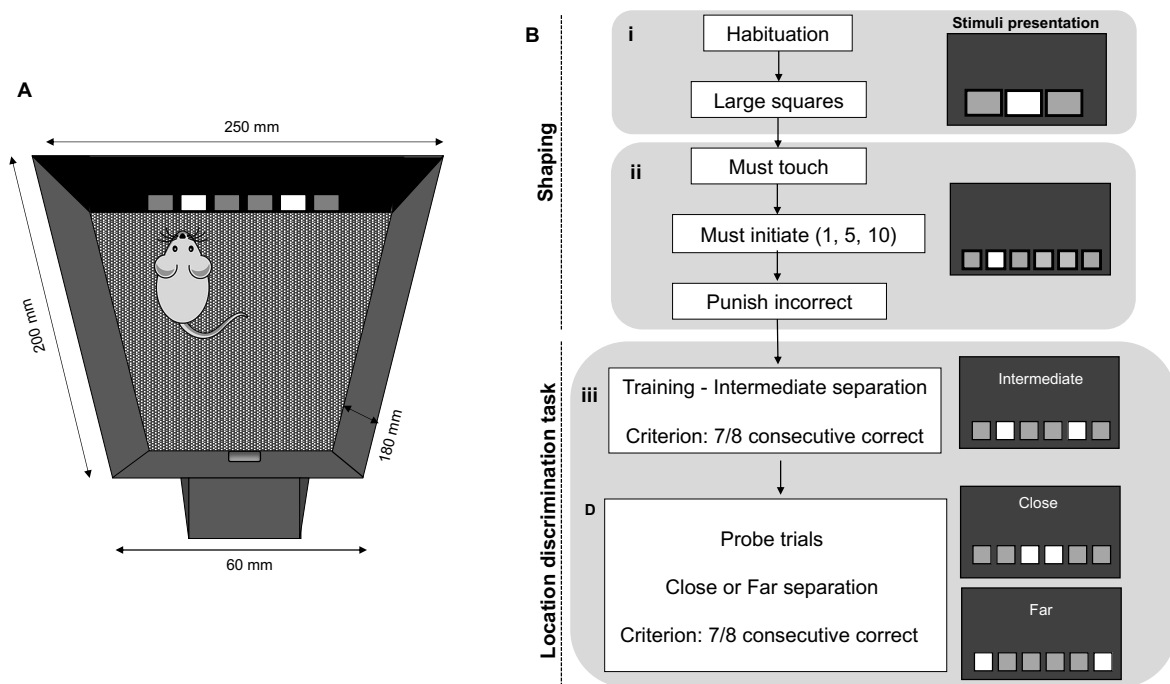
Figure 1. Location discrimination (LD) task. A) Campden Instruments Ltd. mouse

operant touchscreen chamber. The apparatus was housed inside sound-proof, sealed

cubicles. The touchscreen was situated at the front of the chamber and black plastic

masks with apertures were superimposed upon the touchscreen to direct nose pokes

to the appropriate area of the screen on which stimuli were displayed. The mask used

depended on the stage of training (see B). To the rear of the chamber, a magazine

unit was integrated through which measured liquid rewards were delivered. In order to

record the subject's movement, two photo-beams extended between the sidewalls

parallel to the touchscreen and reward delivery area. The chamber floor was a

perforated stainless steel raised above a tray filled with sawdust. **B)** Task structure.

i) The initial stage of shaping consists of habituation and large squares. This stage

teaches subjects to touch the screen to obtain reward. **ii)** The latter half of the shaping

stage trains subjects to responds to smaller stimuli, to self-initiate trials and respond

only to the illuminated stimulus. **Iii)** After fulfilling criteria, subjects began training with

stimuli at an intermediate separation After reaching criterion at intermediate separation

259

260   **2.7.4 Task training**

261   This stage saw the introduction of spatial discriminations, owing to the dual

262   presentation of stimuli on the touchscreen, separated by an intermediate distance

263   (response windows 2 and 5, Figure 1B,iii). One location (e.g., left) was designated as

264   correct, whereas the other illuminated position (e.g., right) was incorrect. Animals were

265   required to complete seven out of eight consecutive trials correct to reach criterion,

266   after which the reward contingencies were reversed so that the previously incorrect

267   location now became correct (Figure 2). Animals then had to achieve seven out of

268   eight correct responses in the new location to attain criterion (reversal). Reward

269   contingencies continued to reverse after each criterion was reached. The reversal

270   element of the task reduces the likelihood that animals develop a side bias or use non-

271   spatial strategies to complete the task[12,48]. Between consecutive sessions (i.e., on

272   subsequent days of training) the correct stimulus position remained consistent (e.g., if

273   a session ended with the left stimulus being rewarded, the subsequent session, on the

274   next day, would also begin with the left stimulus being rewarded). Subjects were

275   considered to have completed training when they were able to achieve twenty trials or

276   more per session, with a minimum of one reversal (i.e., reaching criterion twice) per

277   session, on each of two consecutive days.

278
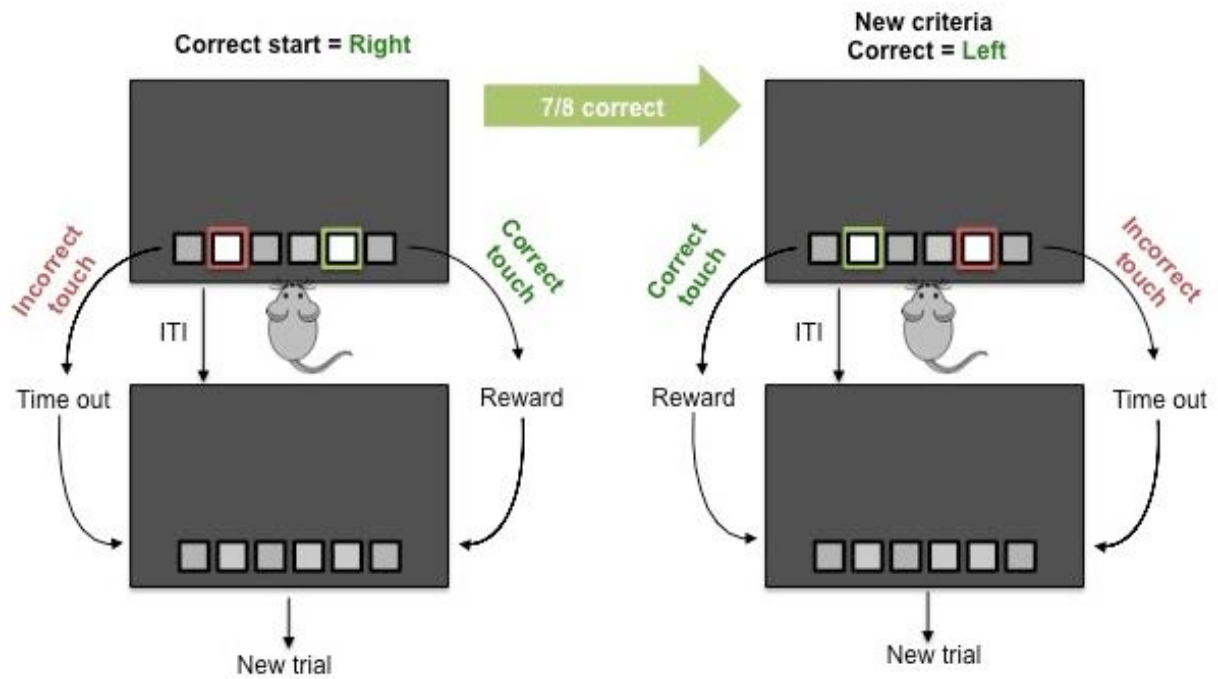
Figure 2. Trial structure for training stage and probe trials. Left panel shows a subject beginning a training session with the right-sided location designated correct. If an incorrect response is made, stimuli disappear and time-out occurs followed by a 10 second ITI, after which a new trial can be initiated. If a correct response is made, stimuli disappear, a reward can be collected and a new trial initiated after a 10 second ITI. If the subject makes 7 correct responses in 8 consecutive trials, the reward contingency is reversed and the left sided stimulus is now rewarded (right panel). The same process then ensues until the subject reaches criteria and another reversal occurs, after which the right side will be rewarded once again.

2.7.5 Probe trials

Having met criteria on the training stage, subjects were advanced to a series of probe sessions (Figure 1B,iii). Trials followed the same structure as the training stage (Figure 2), except for the addition of a spatial discrimination manipulation; sessions featured

294   either far stimulus separations (positions 1 and 6 illuminated) or close stimulus

295   separation (positions 3 and 4 illuminated; Figure 1B,iii). Within one session, all

296   stimulus presentations were either close or far, and each subject received sessions of

297   the same probe type on two consecutive days. The rewarded location did not change

298   between day one and two (unless the subject had finished on a reversal), for example

299   if a subject finished their session on day 1 with the left location being rewarded, they

300   would continue with the left stimulus being rewarded on day 2 until they reached

301   criterion and a reversal occurred. Animals starting on close or far, and with left and

302   right rewarded stimuli, were counterbalanced across groups. Animals received two

303   pairs of probe trials across 4 separate days, with this sequence being repeated twice,

304   meaning that all animals experienced 4 sessions of each separation.

305   **2.7.8 LD task data analysis**

306   For data analysis, all performance metrics including trials to criterion and percentage

307   correct responses to criterion were calculated across all 4 sessions of each separation.

308   In the instance animals did not attain any criteria, which was more common under the

309   close stimuli separation, the number of trials until the completion of probe trials of the

310   same type was substituted to prevent missing data.

311   **2.8 Statistics**

312   All statistical analyses were carried out using GraphPad Prism 8.4.1 (GraphPad

313   Software, CA, USA). Data was assessed for equality of variances using the Brown-

314   Forsythe test and then appropriate parametric (t test, one-way or two-way ANOVA) or

315   non-parametric (Kruskal-Wallis) tests used. The main between-subjects' factor for

316   ANOVA analyses was GENOTYPE (WT, $C3^{-/-}$ or $C3aR^{-/-}$). For morphological analyses,

there was an additional within-subjects factor of BLADE (suprapyramidal, infrapyramidal) and for BrdU long-pulse migration analyses there was a within-subjects factor of BIN (1,2,3,4). For the condensed milk habituation experiment, there was a within-subject factors of SESSION (3-7) and for analysis of LD task probe trial data, there was an additional within-subjects factor of SEPARATION (Close, Far). As we predicted differences in the close but not the far condition, planned comparisons using Tukey posthoc tests were carried out to analyse probe trial performance between genotypes. For migration analyses, planned comparisons were used to compare the proportion of BrdU$^+$ cells between genotypes at each bin. For all other analyses, posthoc pairwise comparisons were performed using the Tukey or Dunn's tests for parametric or non-parametric analyses, respectively. For all analyses, alpha was set to 0.05 and exact p values were reported unless $p < 0.0001$. All p values were multiplicity adjusted[52]. Data are expressed as mean ± standard error of the mean.

3. Results

3.1 Lack of C3/C3aR does not affect progenitor cell proliferation or neuronal fate choice

Wildtype, $C3^{-/-}$ and $C3aR^{-/-}$ mice were injected with thymidine analogue BrdU (100mg/kg, I.P) 6 hours prior to sacrifice, and brain tissue harvested to quantify uptake (Figure 3A). We also co-stained tissue with the endogenous proliferation marker Ki67 (Figure 3B). There were no differences in the total number of BrdU$^+$ cells in the granule cell layer (GCL; Figure 3C) or the total number of Ki67$^+$ cells (Figure 3D), or in the distribution of these cells in dorsal and ventral regions of the hippocampus (Figure S1A). The mitotic index (BrdU$^+$Ki67$^+$/BrdU$^+$) was also unaltered, suggesting no differences in cell cycle speed between genotypes (Figure 3E). Additionally, the area of the GCL (measured in both dentate gyri of each section) was equivalent between genotypes (Figure S2A). We also investigated the location of BrdU-labelled cells within the dentate. In the absence of C3 and C3aR, we did not see any differences in the number of ectopically located (either in the hilus or inner molecular layer) BrdU$^+$ Ki67$^+$ cells (Figure S2B).

A

BrdU

Day 0 ——————————————→ 6 h

B

DAPI | BrdU | Ki67 | Merge

C Total BrdU⁺ cells

D Total Ki67⁺ cells

E Ki67⁺ BrdU⁺ / Ki67⁺
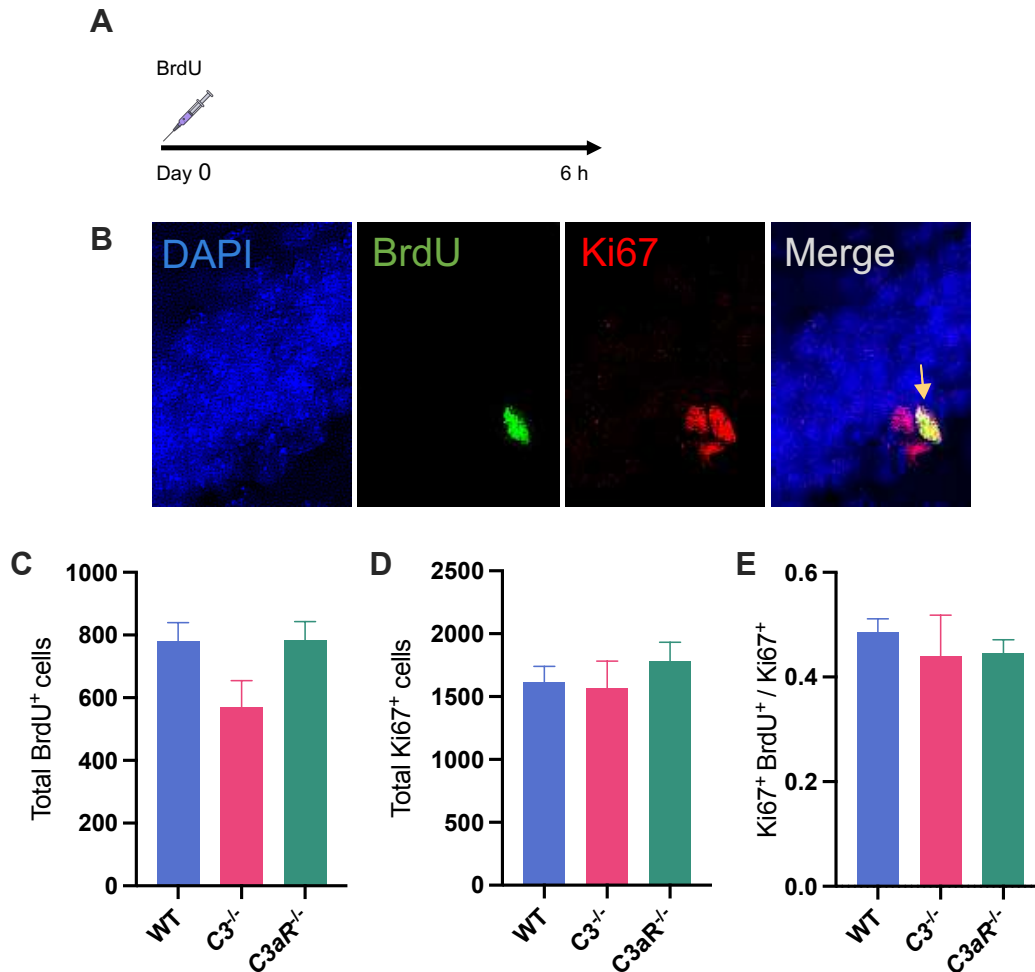
WT, C3⁻/⁻, C3aR⁻/⁻

Figure 3. C3/C3aR deficiency does not impact acute proliferation in the dentate gyrus. (A) Animals were injected with BrdU (100mg/kg, I.P) 6 hours prior to sacrifice, and brain tissue harvested to quantify BrdU uptake. **(B)** Immunohistochemistry was performed for BrdU and Ki67 reactivity. Panel contains representative example of BrdU and Ki67 staining in the granule cell layer. Arrow indicates double positive BrdU⁺ Ki67⁺ cells situated in the sub granular zone. **(C)** Total number of BrdU⁺ cells WT 779.33±60.01, *C3⁻/⁻* 570.00±84.26, *C3aR⁻/⁻* 782.6±60.28; $F_{2,13}$=0.2.87, p=0.6926. **(D)** Total number of Ki67⁺ cells; WT 1614.66±126.94, *C3⁻/⁻* 1568.58±213.25, *C3aR⁻/⁻* 1781.33±151.23; $F_{2,15}$=0.445, p=0.6491. **(E)** Proportion of BrdU⁺ proliferating (Ki67⁺) cells; WT 0.48±0.02, *C3⁻/⁻* 0.43±0.07, *C3aR⁻/⁻* 0.44±0.02; $F_{2,13}$=0.390, p=0.6850. Data are expressed as mean ± S.E.M. Wildtype *N* =6, *C3⁻/⁻ N =4, C3aR⁻/⁻ N =6.*

384   In a separate cohort of animals, we investigated the phenotype of proliferating cells

385   (Ki67$^+$) in the dentate gyrus using the glial marker GFAP and immature neuronal

386   progenitor marker doublecortin (DCX; Figure 4A&E). In this cohort there were again

387   no differences in the total number of Ki67$^+$ cells (Figure 4B). There were no differences

388   in the number of proliferating type 1 cells (Ki67$^+$GFAP$^+$ cells within the GCL with apical

389   morphology; Figure 4C) and these cells accounted for a similar proportion of the total

390   Ki67$^+$ population between genotypes suggesting no differences in the proliferative

391   stem cell pool (Figure 4D). The total number of proliferating type 2b/3 neuronal

392   progenitor cells was also unchanged (Ki67$^+$DCX$^+$; Figure 4F) and these cells again

393   accounted for a comparable proportion of the proliferative population across

394   genotypes (Figure 4G) indicating that early neuronal fate choice was unaffected by

395   absence of C3/C3aR.

396

397   Of the total neuronal progenitor (DCX$^+$) population, significantly fewer of these were

398   in the cell cycle in *C3aR$^{-/-}$* mice compared to wildtype (p=0.0386), whereas *C3$^{-/-}$* mice

399   were unchanged (Figure 4H). Despite a trend towards slight decrease in the total

400   number of DCX$^+$ cells in *C3aR$^{-/-}$* mice (Figure 5A&B) this was not significantly different

401   to WT or *C3$^{-/-}$* mice. Taken together, these findings indicate that the decreased growth

402   fraction of neural progenitor cells in *C3aR$^{-/-}$* mice did not affect the overall production

403   of neural progenitors. There were no genotype differences in the distribution of any of

404   the aforementioned cell types along the hippocampal longitudinal axis (Figure S1 B-

405   D).

406

A DAPI | GFAP | Ki67 | Merge

B Total Ki67$^+$ cells (WT, C3$^{-/-}$, C3aR$^{-/-}$)

C Total Ki67$^+$ GFAP$^+$ cells (WT, C3$^{-/-}$, C3aR$^{-/-}$)

D Ki67$^+$ GFAP$^+$ / Ki67$^+$ (WT, C3$^{-/-}$, C3aR$^{-/-}$)

E DAPI | Ki67 | DCX | Merge

F Total Ki67$^+$ DCX$^+$ cells (WT, C3$^{-/-}$, C3aR$^{-/-}$)

G Ki67$^+$ DCX$^+$ / Ki67$^+$ (WT, C3$^{-/-}$, C3aR$^{-/-}$)

H Ki67$^+$ DCX$^+$ / DCX$^+$ (WT, C3$^{-/-}$, C3aR$^{-/-}$) *

407

18
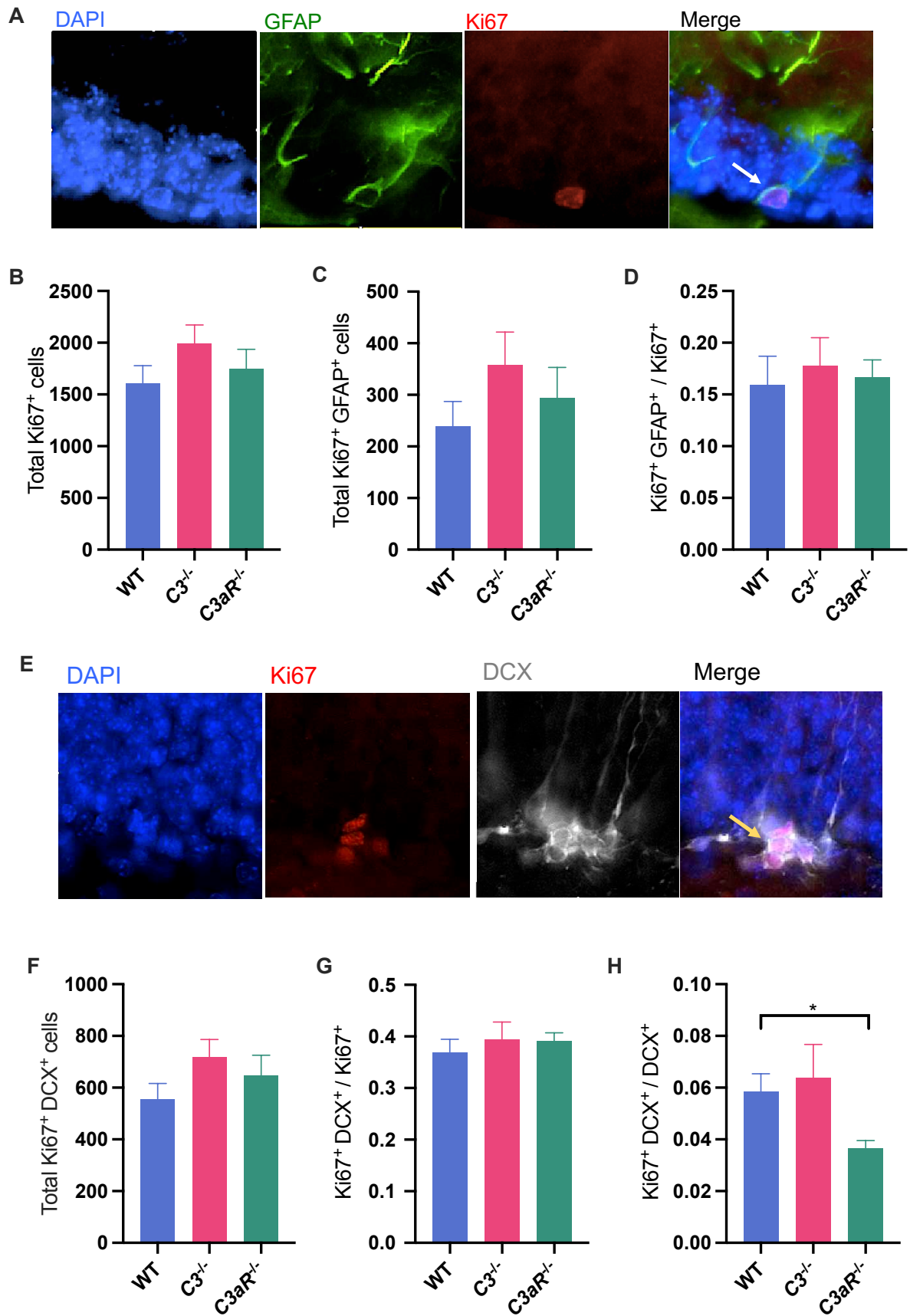
408 **Figure 4. C3/C3aR deficiency does not impact the proliferation of type 1 radial**

409 **glial cells whereas C3aR specifically reduces the proportion of neuroblasts that**

410 **are proliferating.** In a further cohort of animals, immunohistochemistry was

411 performed for Ki67, GFAP and doublecortin (DCX) reactivity. **(A)** Representative

412 example of Ki67 and GFAP staining. Ki67$^+$ GFAP$^+$ cells were only counted if they

413 demonstrated the apical morphology characteristics of type 1 radial glial cells and were

414 situated in the granule cell layer (as indicated by white arrow). **(B)** Total number of

415 Ki67$^+$ cells. WT 1606.00$\pm$172.00, $C3^{-/-}$ 1993.00$\pm$178.6, $C3aR^{-/-}$ 1749.00$\pm$188.7;

416 $F_{2,15}$=1.19, p=0.3321. **(C)** Total number of proliferating type 1 radial glial cells (Ki67$^+$

417 GFAP$^+$); WT 238.50$\pm$48.80, $C3^{-/-}$ 357.90$\pm$63.91, $C3aR^{-/-}$ 292.80$\pm$60.30, $F_{2,15}$=1.06,

418 p=0.3703. **(D)** Proportion of Ki67$^+$ GFAP$^+$ cells in total Ki67$^+$ population; WT 0.15$\pm$0.02,

419 $C3^{-/-}$ 0.17$\pm$0.02, $C3aR^{-/-}$ 0.16$\pm$0.01; $F_{2,15}$=0.143, p=0.8678. **(E)** Representative

420 example of Ki67 and DCX staining. Yellow arrow indicates a cluster of double positive

421 cells. **(F)** Total number of immature neuronal progenitor cells in the cell cycle (Ki67$^+$

422 DCX$^+$). WT 557.10$\pm$58.87, $C3^{-/-}$ 719.00$\pm$67.24, $C3aR^{-/-}$ 647.60$\pm$77.54; $F_{2,15}$=1.41,

423 p=0.2744. **(G)** Proportion of Ki67$^+$ DCX$^+$ cells in total Ki67$^+$ population. WT 0.37$\pm$0.02,

424 $C3^{-/-}$ 0.39$\pm$0.03, $C3aR^{-/-}$ 0.39$\pm$0.01; $F_{2,15}$=0.278, p=0.7614**. (H)** Proportion of Ki67$^+$

425 DCX$^+$ cells in total DCX$^+$ population**.** WT 0.05$\pm$0.006, $C3^{-/-}$ 0.06$\pm$0.01, $C3aR^{-/-}$

426 0.03$\pm$0.007; H_2=7.45, p=0.0172. Data are mean $\pm$ S.E.M. Wildtype N =6, $C3^{-/-}$ N =6,

427 $C3aR^{-/-}$ N =6. *= p$\leq$0.05 for *post-hoc* genotype comparisons.

428

A DAPI DCX

WT

C3$^{-/-}$

C3aR$^{-/-}$

B
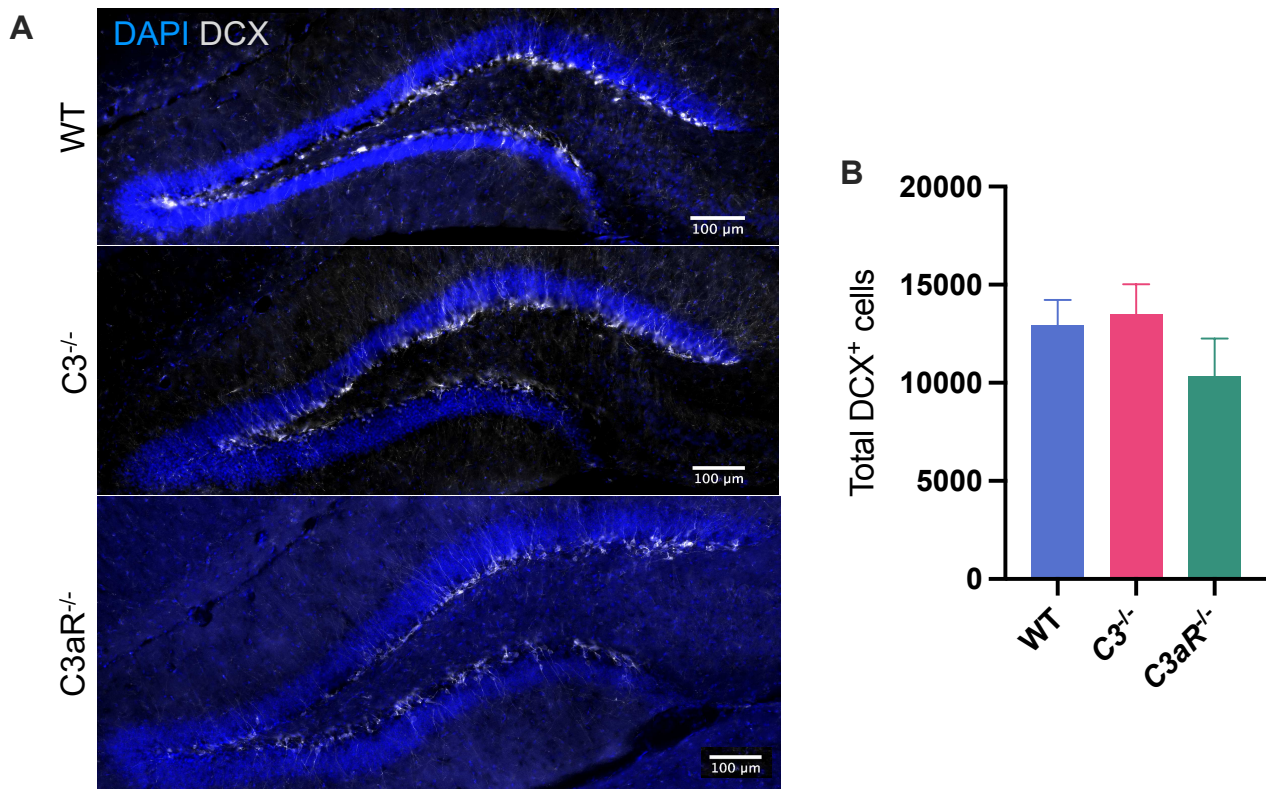
Total DCX$^+$ cells

Figure 5. The total number of immature neuronal progenitor cells is unaffected by lack of C3 and C3aR. (A) Representative example of DCX staining in different genotypes. **(B)** Total number of DCX$^+$ cells. WT 12904±1323, *C3*$^{-/-}$ 13502±1530, *C3aR*$^{-/-}$ 10344±1912; $F_{2,14}$=1.08, p=0.3678. Data are mean ± S.E.M. Wildtype *N* =6, *C3*$^{-/-}$ *N* =5, *C3aR*$^{-/-}$ *N* =6.

3.2 Lack of C3 results in increased neurogenesis due to greater survival of newborn neurons

In order to track the maturation and survival of new neurons born in the dentate gyrus, mice were injected with BrdU (100mg/kg, i.p) daily for 5 days and sacrificed 30 days later (Figure 6A). Tissue was processed for BrdU and NeuN immunoreactivity to detect surviving adult-born neurons (Figure 6B&C). We observed a significantly greater number of BrdU$^+$ cells throughout the hippocampus (Figure S1 E) in *C3*$^{-/-}$ mice compared to both wildtype (p=0.0007) and *C3aR*$^{-/-}$ mice (p=0.0051; Figure 6D). There

444   were also a greater total number of cells double positive for BrdU and NeuN (Figure

445   6E) in $C3^{-/-}$ mice compared to both wildtype (p=0.0022) and $C3aR^{-/-}$ mice (p=0.0139;

446   Figure 6E). The proportion of BrdU labelled cells adopting neuronal fate (BrdU$^+$ NeuN$^+$)

447   was unaltered between genotypes (Figure 6F).

448

449   Given that the total number of proliferating cells (Figure 3), the number of proliferating

450   cells that were expressing DCX (Figure 4F&G) and the proliferation dynamics of

451   immature neurons (Figure 4H) were all unchanged in $C3^{-/-}$ mice, we were confident

452   that there were no changes in early neuronal differentiation or proliferation and

453   therefore the net increase we observed of NeuN$^+$BrdU$^+$ cells in $C3^{-/-}$ mice (Figure 6)

454   suggested a specific effect of C3 on the survival of adult born GCs.

455
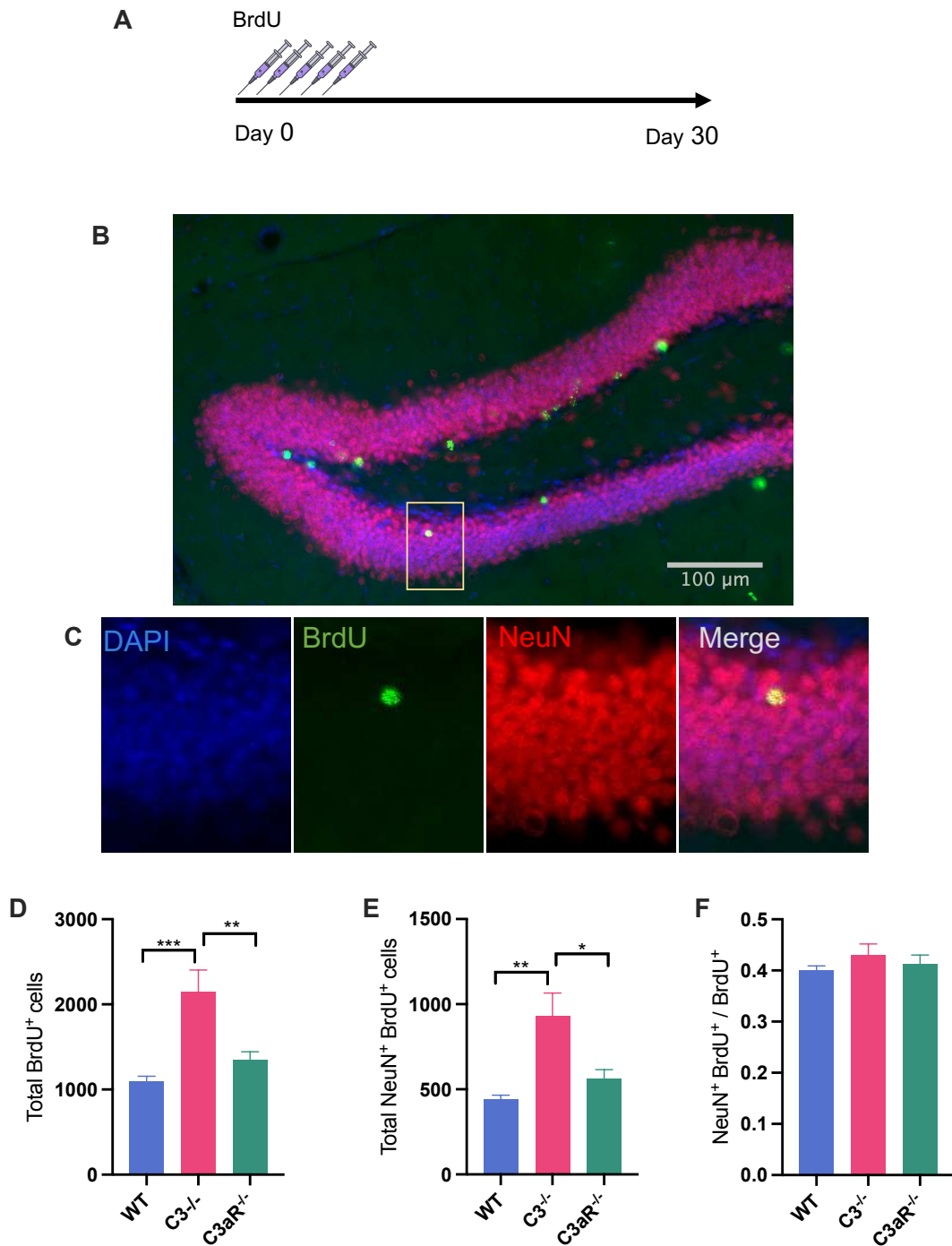
Figure 6. C3 influences the number of surviving adult-born neurons but does not affect fate choice. (A) Animals were injected with BrdU (100mg/kg, I.P) once daily for 5 days and sacrificed 30 days later. **(B)** Brain tissue was sectioned at 40μm and processed for BrdU and NeuN immunoreactivity. Micrograph shows representative staining. Yellow bow indicates example of BrdU$^+$ NeuN$^+$ cell magnified

461   in. **(C)** Representative example of BrdU$^+$ NeuN$^+$ double positive cell. **(D)** Total number

462   of BrdU$^+$ cells. WT 1096±60.9, *C3*$^{-/-}$2152±253, *C3aR*$^{-/-}$ 1344±100, F$_{2,16}$=12.0,

463   p=0.0006. **(E)** Total number of BrdU$^+$ NeuN$^+$ cells. WT 439±26.0, *C3*$^{-/-}$ 932±134, *C3aR*

464    $^{-/-}$ 559±56.5; F$_{2,16}$=9.25, p=0.0021. **(F)** Proportion of total BrdU$^+$ cell population double

465   positive for NeuN$^+$ (neuronal fate). F$_{2,16}$=0.792, p=0.4700. Data are mean ± S.E.M.

466   Wildtype *N* =6, *C3*$^{-/-}$ *N* =6, *C3aR*$^{-/-}$ *N* =7. *, ** and *** represent p≤0.05, p≤0.01 and

467   p≤0.001 for *post-hoc* genotype comparisons, respectively.

468

469   **3.3 Lack of C3 results in accelerated migration of surviving new neurons outside**

470   **the sub granular neurogenic niche**

471   As adult-born neurons mature, they migrate from the sub granular zone (SGZ) deeper

472   into the granule cell layer (GCL)[53] as they extend their apical dendrites further into the

473   molecular layer[54]. To measure the migration of surviving neurons labelled in the 30-

474   day BrdU pulse-chase experiment, we measured the distribution of BrdU$^+$ cells within

475   the GCL. We divided the GCL into four equal bins, the innermost of which

476   corresponded to the SGZ, the band approximately two cell bodies thick that follows

477   the GCL-hilar border. The subsequent two bins (1 & 2) represented the middle layers

478   of the GCL, whereas bin 3 consisted of the outermost portion of the GCL proximal to

479   the inner molecular layer (Figure 7A). There were no significant differences in the

480   thickness of the GCL between wildtype and *C3*$^{-/-}$ mice (p=0.2622) although C3aR$^{-/-}$

481   mice did have a thicker GCL than wildtypes (p=0.0407; Figure S3) by approximately

482   ~3 μm, less than one cell width. We analysed the number of BrdU$^+$ cells that had

483   migrated beyond the SGZ (i.e., occupied bins 1-3) and found that significantly more

484   BrdU$^+$ cells had migrated in *C3*$^{-/-}$ mice compared to wildtype mice (p=0.0009) and

485   *C3aR*$^{-/-}$ mice (p=0.0146; Figure 7B). The proportion of BrdU$^+$ cells that had migrated

was also significantly increased in *C3$^{-/-}$* mice compared to wildtype (p=0.0055) but not

compared to *C3aR$^{-/-}$* mice (p=0.1367; Figure 7C), suggesting that the increased

numbers of migrated cells in *C3$^{-/-}$* mice were not merely due to surplus cells migrating

normally, but instead due to altered migratory patterns of newborn neurons. Since we

anticipated differences in the proportion of cells that migrated in *C3$^{-/-}$* mice, we

conducted planned comparisons of BrdU^{+} cells within the SGZ or bins 1-3. In *C3$^{-/-}$*

mice, we found an exaggerated proportion of cells in bin 1 compared to wildtype

(p=0.0119) and *C3aR$^{-/-}$* mice (p=0.0312) suggesting accelerated migration of surviving

immature GC neurons in the absence of C3.
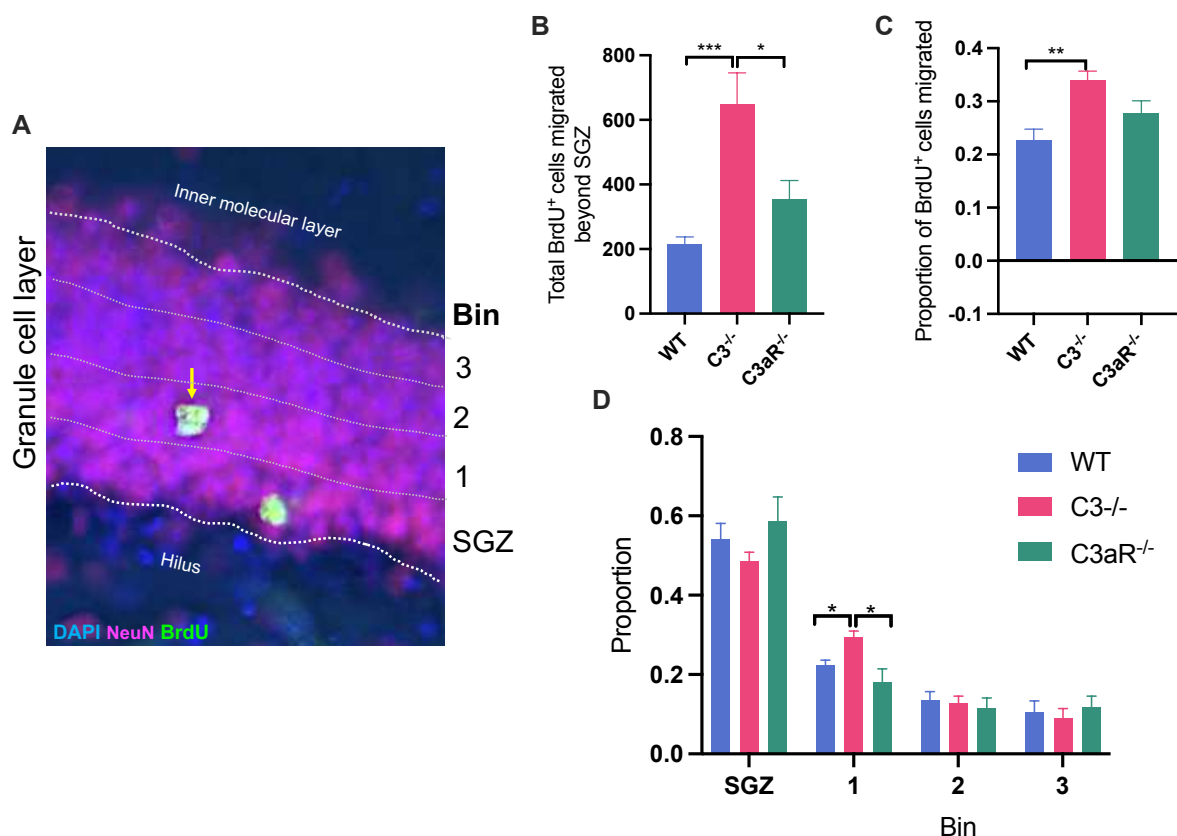
Figure 7. Lack of C3 alters the migration of adult born neurons into the granule cell layer. **(A)** Example of how we divided the GCL into four equal portions or bins. The inner-most bin, proximal to the hilus, compromised the sub granular zone (SGZ).

24

Bin 1 and 2 represented the middle of the GCL, whereas bin 4 represented the outermost layer of the GCL proximal to the inner molecular layer. **(B)** Total number of BrdU⁺ cells that had migrated beyond the SGZ (i.e., in bin 1-3). Wildtype 271±20.8, *C3⁻ᐟ⁻* 648±97.2, *C3aR⁻ᐟ⁻* 356±56.9, $F_{2,16}$=10.8, p=0.0011. **(C)** Migrated cells **(**BrdU⁺ cells found beyond the SGZ) as a proportion of total GCL BrdU⁺ cells. Wildtype 0.22±0.02, *C3⁻ᐟ⁻* 0.34±0.01, *C3aR⁻ᐟ⁻* 0.27±0.02, $F_{2,16}$=7.18, p=0.0059. **(D)** BrdU⁺ cells found in each bin as a proportion of total GCL BrdU⁺ cells. Main effect of BIN; $F_{1.72, 27.5}$=88.1, p<0.0001; GENOTYPE $F_{2,16}$=0.139, p=0.8711; BIN × GENOTYPE $F_{6,48}$=1.51, p=0.1936. Data are mean ± S.E.M. A total of 576 BrdU⁺ cells were analysed from *N=6* wildtype animals, 1139 BrdU⁺ cells from *N=6 C3⁻ᐟ⁻* animals and 869 BrdU⁺ cells from *N =7 C3aR⁻ᐟ⁻* animals. *, ** and *** represent p≤0.05, p≤0.01 and p≤0.001 for *post-hoc* genotype comparisons, respectively.

3.4 Lack of C3/C3aR reduces morphological complexity of immature neuronal progenitor cells

We next used Sholl analysis to investigate the morphology of immature DCX⁺ neurons with vertically oriented apical processes in the GCL. These cells are typically type 3 cells[2], the stage at which the greatest morphological changes occur[53]. Due to the known differences in the dendritic trees of immature neurons located in the suprapyramidal blade versus the infrapyramidal blade of the dentate[55], we analysed cells from each blade separately (Figure 8A). Cells were systematically randomly sampled, and their dendritic trees manually traced and subjected to Sholl analysis (Figure 8B). The resulting Sholl profiles indicated differences in both knockouts in the

25

524   suprapyramidal blade beyond ~70 μm from the cell soma (Figure 8C) but not the

525   infrapyramidal blade (Figure 8D). This was confirmed by analysis of area under the

526   curve, which revealed that both $C3^{-/-}$ and $C3aR^{-/-}$ DCX$^+$ cells had a reduced AUC in

527   the suprapyramidal, but not the infrapyramidal blade, compared to wildtypes (Figure

528   8E).

529   At the outset, these differences could reflect both neurite length and branching[47] and

530   we therefore employed further measures to differentiate these possibilities. The

531   branching index[47] (BI; a specific measure of neurite ramification) of $C3aR^{-/-}$ DCX$^+$ cells

532   was reduced in the suprapyramidal blade compared to that of wildtype and $C3^{-/-}$

533   (Figure 8F) suggesting less complex dendritic branching. In addition, there was a trend

534   towards reduced primary path length of suprapyramidal DCX$^+$ cells in $C3aR^{-/-}$ cells

535   compared to wildtype (Figure S4 A). A similar trend was observed in average branch

536   length (Figure S4 B) and $C3aR^{-/-}$ DCX$^+$ cells had significantly fewer branches

537   compared to wildtype and $C3^{-/-}$ cells, regardless of blade (Figure S4 C). These results

538   indicated an overall reduced dendritic complexity in the absence of C3aR, reflected by

539   decreased branch length, number and ramification in $C3aR^{-/-}$ DCX$^+$ cells.

A

Suprapyramindal blade

Infrapyramidal blade

NeuN

B

DCX   Primary - Branches   Trace

C

Suprapyramidal blade

Number of intersections

Distance from soma (µm)

WT $C3^{-/-}$ $C3aR^{-/-}$

D

Infrapyramidal blade

Number of intersections

Distance from soma (µm)

E

AUC

Supra   Infra

F

Branching Index

Supra   Infra
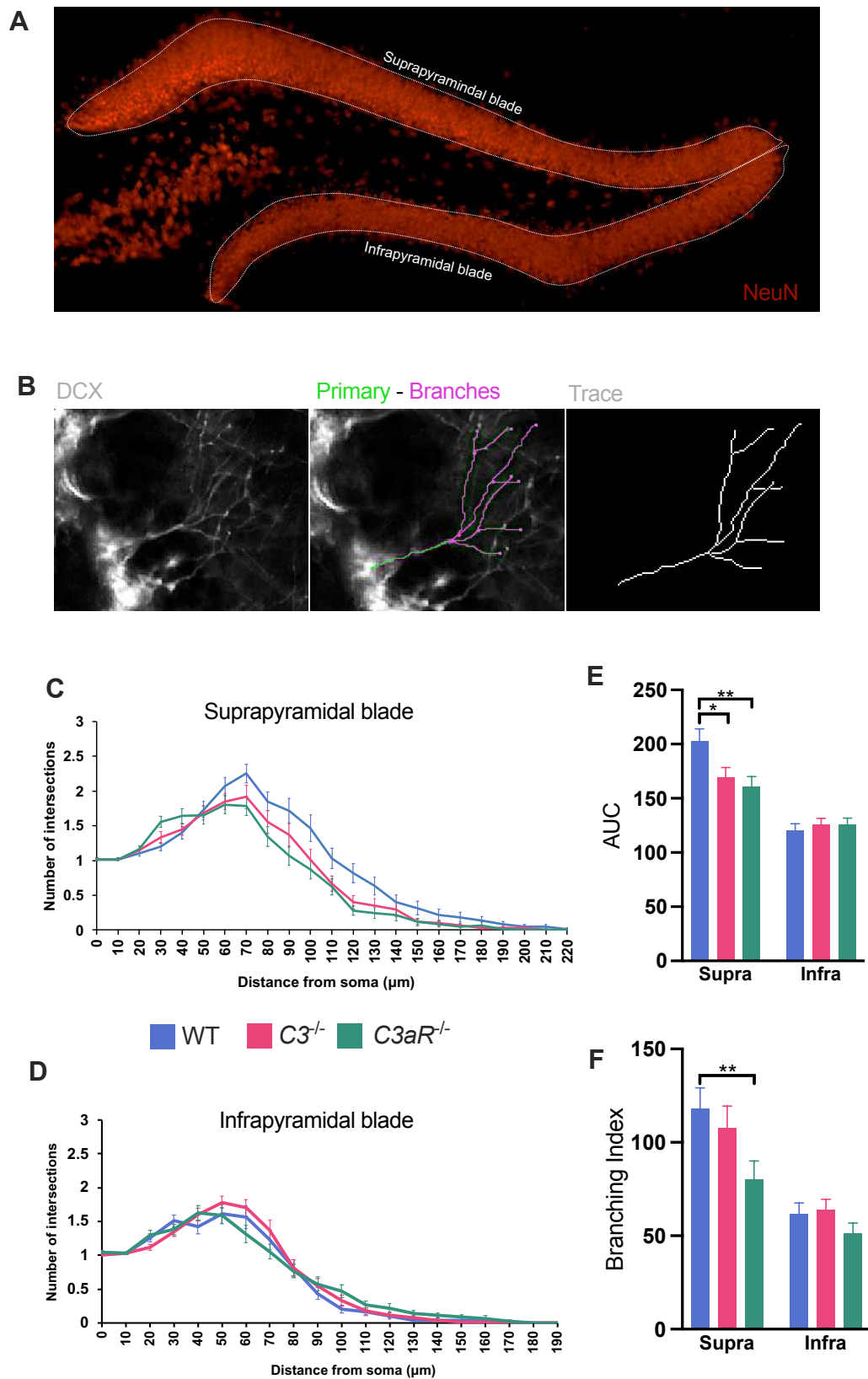
540

541   **Figure 8. Absence of C3/C3aR influences the morphology of immature neurons**.

542   **(A)** Location of suprapyramidal (most dorsal) and infrapyramidal (most ventral) blades.

543   **(B)** Left panel shows a representative example of a DCX^{+} immature neuron selected

544   at random for Sholl analysis. Middle panel shows the tracing in progress, with primary

545   process in green and branches in magenta. Right panel depicts the resulting trace,

546   upon which Sholl analyses are based. **(C)** Sholl curve for cells in suprapyramidal blade

547   **(D)** Sholl curve for cells in infrapyramidal blade. **(E)** Area under the curve (AUC)

548   analysis. WT 202.41±11.74, *C3*$^{-/-}$ 169.41±8.97, *C3aR*$^{-/-}$ 160.91±9.25. BLADE ×

549   GENOTYPE interaction $F_{2,386}=4.68$, p=0.0098 [WT vs. *C3*$^{-/-}$ p=0.0167, WT vs. *C3aR*$^{-}$

550    $^{/-}$ p=0.0017, *C3*$^{-/-}$ vs. *C3aR*$^{-/-}$ p=0.7573] and main effect of BLADE; $F_{1,386}=65.9$,

551   p=<0.0001. **(F)** Branching Index (BI); WT 117.39± 10.88, *C3*$^{-/-}$ 107.39±11.35, *C3aR*$^{-/-}$

552   79.98±9.79; main effect of GENOTYPE $F_{2,272}=4.29$, p=0.0147 *post hoc* WT vs. *C3aR*$^{-}$

553    $^{/-}$ p=0.0076, *C3*$^{-/-}$ vs. *C3aR*$^{-/-}$ p=0.0556, WT vs. *C3*$^{-/-}$ p=0.7494. Data are mean ± S.E.M.

554   Analyses were of 131 cells from *N* =6 wildtype animals, 127 cells from *N* =5 *C3*$^{-/-}$

555   animals*,* and 131 cells from *N* =6 *C3aR*$^{-/-}$ *animals.* * and ** represent p≤0.05 and

556   p≤0.01 respectively for *post-hoc* genotype comparisons.

557

558   Overall, our histological data indicated that lack of C3 specifically increased the

559   survival of adult born neurons and accelerated their migration. Lack of either C3 or

560   C3aR had effects on the morphological development of adult born neurons, though

561   this was more pronounced in the absence of C3aR. We next assessed the functional

562   relevance of these phenotypes for pattern separation, the computational process

563   thought to supported by adult born neurons that is important for distinguishing between

564   similarly encoded spatial or contextual stimuli[8].

565

566

567 **3.5 *C3aR*^{-/-} mice demonstrate improved pattern separation whereas *C3*^{-/-} show**

568 **evidence of impaired cognitive flexibility**

569 We investigated AHN-related behaviours in a reward-based visual discrimination task

570 using a paradigm previously shown to be sensitive to manipulations of AHN in

571 assaying pattern separation[44,50,56]. The task required discrimination of stimuli with

572 varying degrees of spatial proximity with closer stimuli placing a greater demand upon

573 pattern separation[10,12,44]. Mice were initially trained to discriminate the correct

574 response location between two white square stimuli (located in two of six possible

575 locations; Fig 9A) at an intermediate level of spatial separation to a baseline

576 performance criterion of 7 correct responses out of 8. Task difficulty was manipulated

577 from this baseline by introducing probe trials where the stimuli were either further apart

578 (reducing pattern separation requirements) or closer together (increasing pattern

579 separation requirements) than the baseline discrimination (see Fig 9A, probe trials).

580 Prior to beginning training in the touch-screen apparatus, we established equivalent

581 locomotor activity between genotypes (Figure S5A), adapted mice to a water

582 deprivation schedule to motivate reward-orientated behaviour (Figure S5B) and

583 established equal preferences for condensed milk, the liquid foodstuff to be used as

584 reward in the discrimination task (Figure S5C).

585

586 An initial finding was that in the earliest stages of behavioural shaping (Figure S6) and

587 training to baseline criterion (Figure 9B), *C3*^{-/-} mice displayed a relative enhanced

588 performance, requiring fewer trials to reach criterion. Upon reaching baseline

589 performance each animal was subjected to the probe trials. As predicted, task difficulty

590 was increased in the close stimuli separation condition, an effect seen across

591 genotypes as evidenced by an overall reduced percentage of correct responses made

592 in reaching the criterion of 7/8 correct responses (Figure 9D), fewer mean criteria

593 achieved (where the mice could continue responding beyond reaching the first

594 criterion following a reversal of the rewarded stimuli position; Figure 9E) and increased

595 latencies for both correct and incorrect responses (Figure 9H).

596

597 As we anticipated differences in the effects of the close and far probes, we carried

598 out planned comparisons using *posthoc* Tukey tests that revealed an enhanced

599 performance of *C3aR*$^{-/-}$ mice in reaching the first criterion on close probe trials

600 compared to wildtype and *C3*$^{-/-}$ mice. *C3aR*$^{-/-}$ mice were relatively unperturbed by the

601 close separation probe, and under that condition required fewer trials to reach the first

602 criterion compared to both wildtype and *C3*$^{-/-}$ mice (Figure 9C; WT vs C3aR$^{-/-}$

603 p=0.0150, *C3*$^{-/-}$ vs. C3aR$^{-/-}$ p=0.0004). *C3aR*$^{-/-}$ mice also made a greater percentage

604 of correct responses in achieving the first criterion in the close separation probe

605 compared to wildtypes (Figure 9D; WT vs C3aR$^{-/-}$ p=0.0235, *C3*$^{-/-}$ vs. C3aR$^{-/-}$

606 p=0.2673). Although there was a trend towards *C3*$^{-/-}$ mice requiring more trials to reach

607 criterion, their performance was not significantly different to wildtype mice on either

608 the number of trials to first criterion (WT vs. *C3*$^{-/-}$ p=0.3267; Figure 9C) or the

609 percentage of correct responses before achieving first criterion (WT vs. *C3*$^{-/-}$ p=0.5790;

610 Figure 9D). There were no significant differences between genotypes in the far

611 separation condition in either trials to first criterion or percentage correct responses to

612 first criterion (Figure 9C,D).

613

614 After animals reached the first criterion in either the close or far condition, the spatial

615 position of the rewarded stimulus was reversed and relearning of the contingency was

616 required to reach subsequent criteria. In reality animals rarely reached criterion within

617   the same session especially under the close condition, so we took account of all probe

618   trial sessions of each separation type to calculate the mean number of criteria

619   achieved. Mirroring to an extent the enhanced performance of $C3^{-/-}$ mice at the

620   baseline training stage (Figure 9B), where stimuli were separated by an intermediate

621   distance, $C3^{-/-}$ mice achieved significantly more criteria across sessions than wildtype

622   and $C3aR^{-/-}$ mice under the far separation (Figure 9E; C3$^{-/-}$ vs. WT p=0.0001, vs. C3aR$^{-/-}$

623     $^{-/-}$ p=0.0019,) but not however at the close separation ($C3^{-/-}$ vs WT p=0.3077; vs. $C3aR^{-/-}$

624     $^{-/-}$ p=0.6302). This was an important distinction since it implied that the apparent

625   enhanced performance in the far separation condition was not due to an effect on

626   pattern separation, since any advantage would be manifest in the close but not far

627   separation condition.

628

629   We observed that the behaviour of the $C3^{-/-}$ mice was characterised by a general

630   increase in responding resulting in a significantly greater number of trials across all

631   sessions regardless of stimulus separation (Figure 9F). We also noted that $C3^{-/-}$ mice

632   showed a different response style compared to wildtype and $C3aR^{-/-}$ mice,

633   demonstrating decreased response latencies, regardless of accuracy or stimulus

634   separation, although these differences were particularly pronounced at close

635   separations due to the slowing of responses in wildtype and $C3aR^{-/-}$ mice (Fig 9H;

636   correct responses at close $C3^{-/-}$ vs. WT p=0.1126; vs. C3aR$^{-/-}$ p=0.0295; and incorrect

637   responses at close $C3^{-/-}$ vs. WT p=0.0011 vs. C3aR$^{-/-}$ p=0.0133). In addition, $C3^{-/-}$ mice

638   made a greater number of inter-trial interval touches across conditions (Figure 9I;

639   Close; $C3^{-/-}$ vs. WT p=0.0073; vs. $C3aR^{-/-}$ 3p=0.0025; Far $C3^{-/-}$ vs. WT p=0.0039, vs.

640     $C3aR^{-/-}$ p=0.0150).

641

642   The pattern of behaviour in the *C3*$^{-/-}$ mice was reminiscent of impaired behavioural

643   inhibition, that is, a relative inability to suppress inappropriate responding. To test this

644   further we took advantage of the reversal manipulation component of the paradigm

645   and analysed the number of incorrect responses made post-reversal as an index of

646   perseverative responding having first adjusted this for the number of criteria achieved

647   per subject. We found that *C3*$^{-/-}$ mice made significantly more perseverative errors per

648   criteria when stimuli were close together (Figure 9G; *C3*$^{-/-}$ vs. WT p=0.0008, vs. *C3aR*$^{-}$

649    $^{/-}$ p=0.0142) but not far apart (*C3*$^{-/-}$ vs. WT p=0.6512, vs. *C3aR*$^{-/-}$ p=0.8060). These

650   data were consistent with a deficit in behavioural inhibition manifest under conditions

651   of increased task difficulty where there were increased demands on pattern

652   separation.

653

654   In summary*, C3aR*$^{-/-}$ showed enhancements in pattern separation abilities, evidenced

655   by improved discrimination performance under conditions where stimuli were highly

656   spatially similar. In contrast, *C3*$^{-/-}$ behaviour was consistent with deficits in cognitive

657   flexibility arising from impaired behavioural inhibition that were especially marked

658   under conditions of increased task difficulty.

659
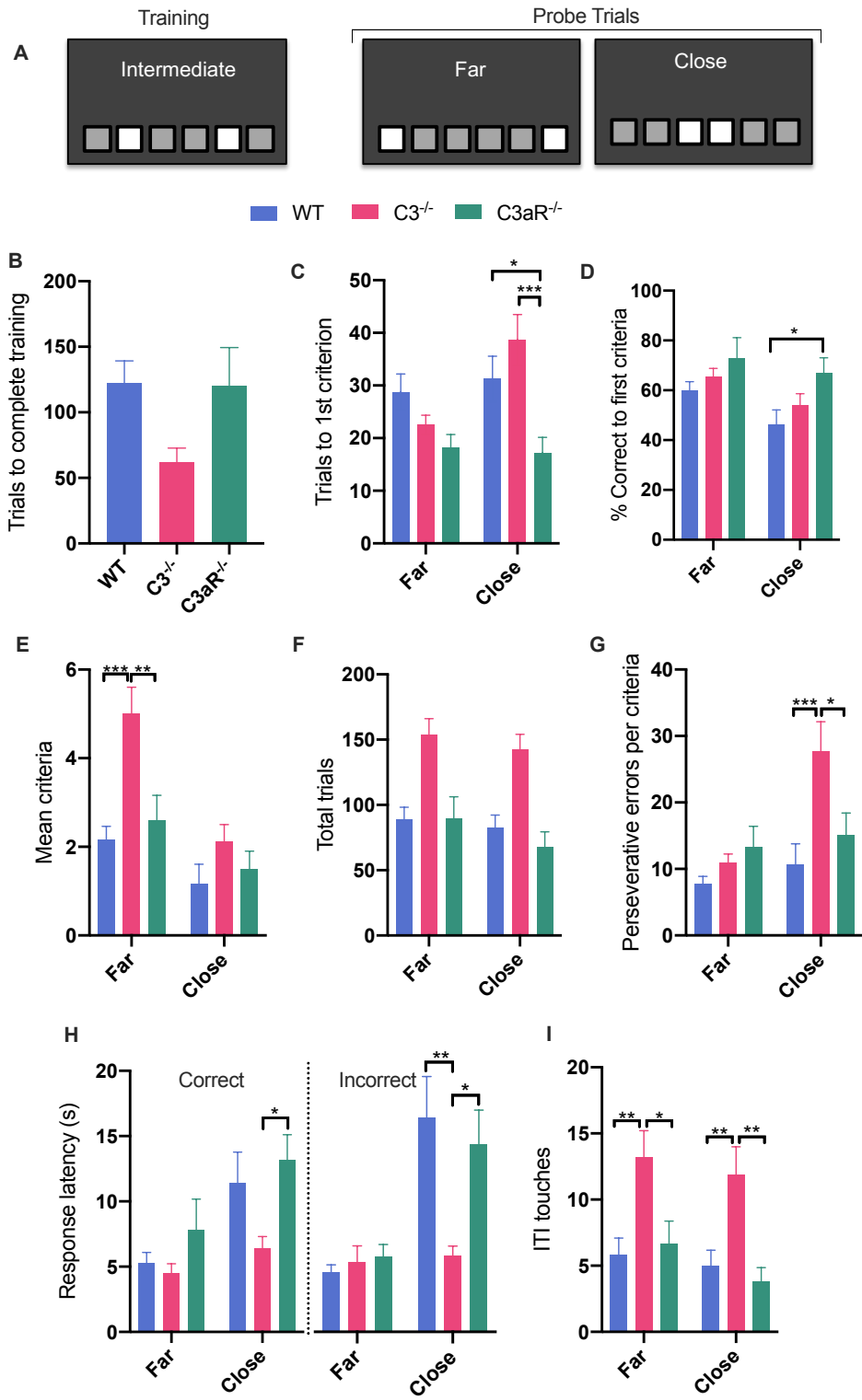
Figure 9. Performance on the location discrimination task. (A) Subjects were first trained on stimuli separated by an intermediate distance, before moving onto probe trials in which the spatial separation between stimuli was manipulated to tax pattern separation. Criteria was reached when subjects made 7 out of 8 correct responses on

665 consecutive trials, after which the reward contingency was reversed, and subjects

666 were required to re-learn the contingency to achieve a subsequent criterion. **(B**) Mean

667 number of trials needed to complete training. H_2=5.59, p=0.0610. **(C)** Trials to first

668 criterion. Planned comparison of genotypes at close; WT 31.08±4.31 vs *C3aR$^{-/-}$*

669 17.00±2.93 p=0.0150, *C3$^{-/-}$* 38.33±4.87 vs. *C3aR$^{-/-}$* p=0.0004, WT vs. *C3$^{-/-}$* p=0.3084

670 and far; WT 28.50±3.43 vs *C3aR$^{-/-}$* 17.90±2.47 p=0.0851, *C3$^{-/-}$* 22.17±1.82 vs. *C3aR$^{-/-}$*

671 p=0.6957, WT vs. *C3$^{-/-}$* p=0.4238. **(D)** Percentage of correct responses made in the

672 run up to first criterion; main effect of SEPARATION $F_{(1,28)}$=4.64, p=0.0400. Planned

673 comparisons of genotypes at close: WT 46.16±5.98 vs *C3aR$^{-/-}$* 67.03±6.05 p=0.0235,

674 *C3$^{-/-}$* 54.08±4.55 vs. *C3aR$^{-/-}$* p=0.2673 and far; WT 60.04±3.44 vs *C3aR$^{-/-}$* 72.86±8.29

675 p=0.7731, *C3$^{-/-}$* 65.46±3.34 vs. *C3aR$^{-/-}$* p=0.6440, WT vs. *C3$^{-/-}$* p=0.7731. **(E)** Mean

676 criteria achieved across sessions; main effect of SEPARATION $F_{(1,28)}$=49.5, p<0.0001.

677 Planned comparisons at close; *C3$^{-/-}$* 1.06±0.19 vs WT 0.54±0.20 p=0.3077; vs. *C3aR$^{-/-}$*

678 0.75±0.20 p=0.6302; WT vs. *C3aR$^{-/-}$* p=0.8528 and far; *C3$^{-/-}$* 5.11±0.63 vs WT

679 2.17±0.30 p=0.0001, vs. *C3aR$^{-/-}$* 2.60±0.56 p=0.0019, WT vs. *C3aR$^{-/-}$* p=0.7646. **(F)**

680 Total trials completed across sessions. Close WT 82.67±9.60, *C3$^{-/-}$* 142.78±11.31,

681 *C3aR$^{-/-}$* 67.70±11.75; Far WT 89.08±9.16, *C3$^{-/-}$* 153.56±12.60, *C3aR$^{-/-}$* 89.60±16.73.

682 Main effect of GENOTYPE; $F_{(2,28)}$=10.6, p=0.0004 [*posthoc C3$^{-/-}$* vs WT p=0.0015;

683 vs. *C3aR$^{-/-}$* p=0.0007; WT vs. *C3aR$^{-/-}$* p=0.8877]. **(G)** The number of perseverative

684 errors (incorrect responses made after a reversal) were calculated and adjusted to

685 account for differences in the number of criteria reached per animal. Planned

686 comparisons at close; *C3$^{-/-}$* 27.64±4.52, vs. WT 10.71±3.09 p=0.0008, vs. *C3aR$^{-/-}$*

687 15.07±3.34 p=0.0142; and far *C3$^{-/-}$* 10.91±1.32, vs. WT 7.81±1.09; p=0.6512, vs.

688 *C3aR$^{-/-}$* 13.30±3.11 p=0.8060. **(H)** Latencies of correct and incorrect responses.

689 Correct response latencies; main effect of SEPARATION $F_{(1,28)}$=13.9, p=0.0009;

690 Incorrect response latencies; main effect of SEPARATION $F_{(1,28)}$=18.3, p=0.0002.

691 Planned comparison of correct responses at close *C3*$^{-/-}$ 6.35±0.95 s, vs. WT

692 11.42±2.35 s; p=0.1126; vs. *C3aR*$^{-/-}$ 13.16±1.95 p=0.0295; WT vs. C3aR$^{-/-}$ p=0.7531

693 and incorrect responses at close *C3*$^{-/-}$ 5.57±0.68 s, vs. WT 15.62±3.01 s; p=0.0011;

694 vs. *C3aR*$^{-/-}$ 13.66±2.52 p=0.0133; WT vs. *C3aR*$^{-/-}$ p=0.7278. **(I)** Touches made to the

695 screen in the inter-trial interval (ITI). Planned comparisons at close; *C3*$^{-/-}$ 11.86±2.13

696 s, vs. WT 4.96±1.22 s; p=0.0073; vs. *C3aR*$^{-/-}$ 3.83±1.03 p=0.0025; WT vs. *C3aR*$^{-/-}$

697 p=0.8558; and far *C3*$^{-/-}$ 13.22±1.98, vs. WT 5.83±1.26 s; p=0.0039, vs. *C3aR*$^{-/-}$

698 6.63±1.75 p=0.0150; WT vs. *C3aR*$^{-/-}$ p=0.9267. Data are mean ± S.E.M. *N=12* wildtype

699 animals, *N=9 C3*$^{-/-}$ animals and *N=10 C3aR*$^{-/-}$ animals. *, ** and *** = p≤0.05, p≤0.01

700 and p≤0.001 for *post-hoc* genotype comparisons respectively.

701

702

703

704

705

706

707

708

709

710

711

712

713

4. Discussion

Using knockout mouse models, we conducted an investigation of the impact of signalling through the C3a/C3aR axis on adult hippocampal neurogenesis and demonstrated separable effects of these proteins in regulating cellular, morphological and functional aspects of neurogenesis. C3 impacted upon the survival and migration of new neurons in the GCL, and while both C3 and C3aR influenced the morphology of immature neurons, the effect was most evident in the total absence of C3aR signalling. Lack of C3aR enhanced pattern separation without influencing other aspects of cognition probed in the discrimination task, whereas the increased neurogenesis and altered migration seen in *C3*^{-/-} mice was associated with impairments in cognitive flexibility under conditions placing demands upon pattern separation.

Our findings of enhanced survival in absence of C3 align with a prior report focusing on C3d/CR2 signalling[36]. Consideration of these findings alongside ours may provide clues as to the specific pathways responsible for C3 effects upon cell survival. Moriyama et al (2011)[36] demonstrated an inhibitory role for the C3d/CR2 axis in AHN, reporting increases in immature GCs (BrdU[+] NeuN[+]) in CR2^{-/-} mice using a pulse-chase paradigm equivalent to our own. Our observation of increased basal neurogenesis in *C3*^{-/-} mice but not *C3aR*^{-/-} mice is consistent with this since C3d is derived from C3, thus *C3*^{-/-} mice lack C3d/CR2 signalling whereas *C3aR*^{-/-} mice do not. This suggests that the survival effects we have seen may be due to a lack of signaling through CR2, which under physiological conditions is expressed on neural progenitor cells[36]. Since other C3 breakdown products and their receptors, including C5a/C5aR[57], C3b/CR3[36] and according to our data C3a/C3aR, do not modulate net

36

739 levels of adult neurogenesis[36,], it is likely that C3d/CR2 signalling constitutes a novel

740 immune mechanism to maintain homeostatic levels of neurogenesis.

741   Our findings seem at odds with another report which showed a positive role for

742 the C3a/C3aR axis in regulating adult neurogenesis, evidenced by reduced numbers

743 of neural progenitors (BrdU$^+$ DCX$^+$ cells) and committed immature GCs (BrdU$^+$ NeuN$^+$)

744 in both $C3^{-/-}$ and $C3aR^{-/-}$ mice and wildtype mice treated with a C3aR antagonist[35].

745 While we did see a significant decrease in BrdU$^+$ DCX$^+$ cells in C3aR$^{-/-}$ mice compared

746 to wildtypes, this was not seen in $C3^{-/-}$ mice and our main finding of increased

747 neurogenesis (BrdU$^+$ NeuN$^+$ cells) is inconsistent with these results. However, the use

748 of different pulse-chase intervals in the previous study makes interpretation

749 challenging in terms of disentangling their effects on early progenitor proliferation

750 dynamics versus our effects on neuronal survival. Moreover, a subsequent study from

751 the same group using C3a-overpressing mice did not support a positive role for

752 C3a/C3aR signalling in regulating basal neurogenesis[57]. Instead, our work using both

753 a short-term and a long-term labelling procedure permits clear dissociation of effects

754 on acute proliferation versus long-term survival, demonstrating a prominent role for C3

755 fragments in negatively regulating survival without affecting proliferation or neuronal

756 lineage commitment.

757   The mechanisms through which C3 may influence cell survival are unclear.

758 Only a small percentage of newborn cells are incorporated into the hippocampal

759 circuitry and ~70% are eliminated at the immature neuron stage[61,62] via apoptosis-

760 coupled microglial phagocytosis. One possibility is that C3 signalling promotes

761 programmed cell death, either via cell-intrinsic or extrinsic mechanisms. Similar

762 mechanisms have been described for other complement factors implicated in

763 developmental neurogenesis[87]. Another possibility relates to opportunities for synaptic

764 integration. During development, programmed cell death is necessary for optimal

765 matching of the neuronal population with available synaptic targets[58] and this is

766 recapitulated within the adult neurogenic niche, where important determinants of

767 survival include the success of immature GCs in forming synaptic contacts within the

768 molecular layer. Increased synapse density has been found in this area of the *C3*^{-/-}

769 brain[38,59], presumably due to the absence of normal complement-mediated

770 developmental synaptic elimination[23]. It is therefore possible that increased survival of

771 newborn cells in *C3*^{-/-} mice is facilitated by increased availability of synaptic contacts,

772 less competition and greater opportunity for integration and survival. The accelerated

773 migration of BrdU-labelled cells we observed in *C3*^{-/-} mice is consistent with this

774 notion, since migration into the GCL permits maturation via further reaching synaptic

775 contacts[53].

776   We also demonstrated effects of C3 and C3aR on the morphological complexity

777 of neuronal progenitor cells. Our results, showing reduced dendritic arborisation

778 primarily in the absence of C3aR, support prior *in vitro* studies implicating a necessary

779 role for C3aR in normal neuronal morphology[39,42,43] and is the first to demonstrate this

780 relationship is maintained *in vivo*, within the adult neurogenic niche. While these

781 previous studies have mostly focused on either inhibition of C3aR, or addition of C3a,

782 the fact that our effects were most pronounced in the absence of C3aR suggests

783 redundancy of C3a in mediating morphological development. One possible

784 explanation is that VGF-deprived peptide TLQP-21, a known C3aR ligand[60,61],

785 contributes to the maturation of immature neurons in the hippocampal neurogenic

786 niche, and further investigations are required to address this possibility. Interestingly,

787 we found effects of C3/C3aR on the morphology of neurons in the suprapyramidal, but

788 not infrapyramidal blade. How such specificity might come about is unclear and there

789   is scarce information relating to the transverse hippocampal axis. In a small number

790   of studies that have examined the two blades, differential neurogenesis, in addition to

791   connectivity, dendritic tree size and synapse density of GC neurons has been

792   demonstrated[62-64]. Functionally, although suprapyramidal GCs are known to respond

793   preferentially to spatial exploration[65,66], how their morphology contributes to the

794   functional properties of immature neurons in encoding spatial information is unknown.

795   To assess whether the changes we observed in AHN were associated with

796   functional changes in pattern separation, we used an established discrimination task

797   previously utilised to detect changes in pattern separation after pro-neurogenic[44] and

798   anti-neurogenic manipulations[10,12,49]. Typically, enhancing adult neurogenesis is

799   associated with improved ability to discriminate highly similar stimuli or contexts[44,67,68]

800   although this has not been entirely consistent across the literature[69,70]. Despite

801   increased levels of neurogenesis, $C3^{-/-}$ mice showed impairments in spatial

802   discrimination performance, but only post-reversal, indicating impairments in cognitive

803   flexibility as opposed to pattern separation per se. Interestingly, it has been reported

804   that manipulations of neurogenesis only affected performance on trials after a learned

805   discrimination was reversed, rather than during the initial spatial discrimination[14].

806   Additionally, abnormally enhanced neurogenesis in $C3^{-/-}$ mice may be responsible for

807   impairments in cognitive flexibility. Consistent with our data in $C3^{-/-}$ mice showing

808   elevated levels of neurogenesis alongside impaired reversal learning in the face of

809   increased spatial discrimination demands, ablating neurogenesis has led to

810   improvements in spatial working memory when animals were required to discriminate

811   highly similar cues presented in short succession or when animals needed to suppress

812   conflicting responses[71], conditions akin to our task.

813   Despite the impaired performance of *C3⁻/⁻* mice in the reversal element of the

814   task, *C3⁻/⁻* mice paradoxically achieved the greatest number of criteria (and thus

815   reversals) across groups. We believe this is an epiphenomenon due to these mice

816   completing a greater number of trials throughout training and probe trials. These mice

817   therefore had more opportunity than other groups to reach criterion, even if achieved

818   in a less efficient manner. In the absence of a general hyperactivity phenotype, this

819   may indicate changes in motivation for reward. Moreover, decreased response

820   latencies and increased inappropriate responding in *C3⁻/⁻* indicated a failure of

821   behavioural inhibition and a potential impulsivity phenotype. It is unlikely that

822   increased speed of responding was due to a decreased perceived difficulty of the task

823   for these animals, given that their accuracy of responding was not improved. Using

824   tasks designed to specifically probe the influence of C3 on cognitive flexibility,

825   motivational behaviour and impulsivity will be a priority for future work.

826   *C3aR⁻/⁻* mice on the other hand were superior in their pattern separation ability

827   and were unimpaired by the reversal component of the task. If the cellular phenotypes

828   we have observed in these mice are linked to behavioural phenotypes, it seems

829   paradoxical that decreased morphological complexity of immature neurons in the

830   suprapyramidal blade would benefit function. Indeed, spatial learning has been shown

831   to increase dendritic complexity of immature neurons[72]. While it is known that younger

832   neural progenitor cells mediate pattern separation[73], it has also been demonstrated

833   that less morphologically complex immature DCX cells may be more important for

834   pattern separation and cognitive flexibility than more mature DCX cells and GC

835   neurons (BrdU⁺ NeuN⁺)[74]. Additional factors likely of relevance include the fact that

836   C3aR is also part of a signalling pathway that mediates synaptic strength[75,76] which

837   likely influences the synaptic connectivity both within and beyond the neurogenic

838 niche, consistent with evidence of altered cognition in *C3aR*^{-/-} mice from a variety of

839 contexts[26,39,77,78].

840   An important consideration is our use of constitutive knockouts. Knocking out

841 complement components such as C1q, C3 or CR3 results in sustained deficits in

842 synaptic connectivity[23,33,38,79] which may alter the wider environment in which adult

843 neurogenesis takes place. Furthermore, increased neurogenesis is not always

844 beneficial and is often associated with abnormal neuronal maturation, integration[80]

845 and migration, as we have seen. Therefore, despite the increased levels of

846 neurogenesis we report in *C3*^{-/-} mice, it is possible that their surplus adult born neurons

847 integrate into altered hippocampal circuit and this may have greater effects on

848 cognition than the impacts on GC survival per se.

849   Limitations of our study include our initial focus on male subjects due to known

850 fluctuations in AHN attributable to sex hormones[81]. Given important sexual

851 dimorphism in hippocampal cognition[82] and complement activity[48], this will be a priority

852 in our future work. Finally, we had to adapt our analysis of the location discrimination

853 task due to the considerable difficulty subjects experienced in reaching criterion within

854 a single session, a known challenge of this task when applied in mice as opposed to

855 rats[10,12,44,49]. Instead, we analysed performance across rather than within sessions of

856 each condition and as such there is likely to be more variability in our data introduced

857 by delays between individual sessions than in some other reports[10,12,44,49].

858   In conclusion, we show novel, negative regulatory roles for complement C3 and

859 C3aR in the survival and morphology of adult born neurons in the adult hippocampus,

860 findings consistent with the detrimental impact of excessive inflammation on

861 neurogenesis in neuropathologies such as temporal lobe epilepsy, where complement

862 activation is associated with chronically reduced neurogenesis[83-85]. We demonstrate

863 for the first time that C3 and C3aR influence neurogenesis-associated cognitive

864 processes of relevance to a range of neuropsychiatric disorders in which abnormal

865 neurogenesis and complement activity are implicated[28,86] and add to the growing body

866 of evidence literature demonstrating intriguing non-canonical roles of complement in

867 the brain.

868
869
870
871 **Author contributions**

872 The study was designed by LJW, TH, BPM, MZ, WPG and LSW. LJW and TH

873 performed behavioural experiments. Molecular analyses were performed by LJW, NH,

874 CE and OM. Data interpretation were carried out by LJW, JH, NH, TRH, MZ, BPM,

875 LSW, TH and WPG. The manuscript was drafted by LJW, TH, WPG and LSW. All

876 authors approved the final manuscript.

877

888

889

Competing financial interests

The authors declare no competing financial interests.

Materials and correspondence

All data from this study are available from the corresponding authors upon reasonable request.

References

1. Doetsch, F. A niche for adult neural stem cells. *Current Opinion in Genetics & Development* **13,** 543–550 (2003).
2. Kempermann, G., Jessberger, S., Steiner, B. & Kronenberg, G. Milestones of neuronal development in the adult hippocampus. *Trends Neurosci.* **27,** 447–452 (2004).
3. Kuhn, H. G. Control of Cell Survival in Adult Mammalian Neurogenesis. *Cold Spring Harbor Perspectives in Biology* (2015).
4. Ge, S. *et al.* GABA regulates synaptic integration of newly generated neurons in the adult brain. *Nature* **439,** 589–593 (2006).
5. Anacker, C. & Hen, R. Adult hippocampal neurogenesis and cognitive flexibility - linking memory and mood. *Nat. Rev.* **18,** 335–346 (2017).
6. Kheirbek, M. A. & Hen, R. Add neurons, subtract anxiety. *Sci. Am.* **311,** 62–67 (2014).
7. Kempermann, G. Functional significance of adult neurogenesis. *Current Opinion in Neurobiology* **14,** 186–191 (2004).
8. Yassa, M. A. & Stark, C. E. L. Pattern separation in the hippocampus. *Trends Neurosci.* **34,** 515–525 (2011).
9. Schmidt, B., Marrone, D. F. & Markus, E. J. Disambiguating the similar: The dentate gyrus and pattern separation. *Behav. Brain Res.* **226,** 56–65 (2012).
10. Clelland, C. D. *et al.* A functional role for adult hippocampal neurogenesis in spatial pattern separation. *Science* **325,** 210–213 (2009).
11. Tronel, S. *et al.* Adult-born dentate neurons are recruited in both spatial memory encoding and retrieval. *Hippocampus* n/a–n/a (2015). doi:10.1002/hipo.22468
12. Coba, M. P. *et al.* TNiK is required for postsynaptic and nuclear signaling pathways and cognitive function. *J. Neurosci.* **32,** 13987–13999 (2012).
13. Garthe, A., Roeder, I. & Kempermann, G. Mice in an enriched environment learn more flexibly because of adult hippocampal neurogenesis. *Hippocampus* (2015). doi:10.1002/hipo.22520

930 14. Swan, A. A. *et al.* Characterization of the role of adult neurogenesis in
931   touch-screen discrimination learning. *Hippocampus* **24,** 1581–1591
932   (2014).
933 15. Anacker, C. & Hen, R. Adult hippocampal neurogenesis and cognitive
934   flexibility — linking memory and mood. *Nat. Rev.* **18,** 335–346 (2017).
935 16. Burghardt, N. S., Park, E. H., Hen, R. & Fenton, A. A. Adult-born
936   hippocampal neurons promote cognitive flexibility in mice. *Hippocampus*
937   **22,** 1795–1808 (2012).
938 17. Seib, D. R., Espinueva, D. F., Floresco, S. B. & Snyder, J. S. A role for
939   neurogenesis in probabilistic reward learning. *Behavioral Neuroscience*
940   **134,** 283–295 (2020).
941 18. Ekdahl, C. T., Claasen, J.-H., Bonde, S., Kokaia, Z. & Lindvall, O.
942   Inflammation is detrimental for neurogenesis in adult brain. *Proc. Natl.*
943   *Acad. Sci. U.S.A.* **100,** 13632–13637 (2003).
944 19. Monje, M. L., Toda, H. & Palmer, T. D. Inflammatory blockade restores
945   adult hippocampal neurogenesis. *Science* **302,** 1760–1765 (2003).
946 20. Morley, B. J. & Walport, M. J. *The Complement FactsBook.* (Academic
947   Press, 1999).
948 21. Sayah, S., Ischenko, A. M., Zhakhov, A., Bonnard, A.-S. & Fontaine, M.
949   Expression of Cytokines by Human Astrocytomas Following Stimulation
950   by C3a and C5a Anaphylatoxins. *Journal of Neurochemistry* **72,** 2426–
951   2436 (2002).
952 22. Coulthard, L. G. & Woodruff, T. M. Is the Complement Activation Product
953   C3a a Proinflammatory Molecule? Re-evaluating the Evidence and the
954   Myth. *J. Immunol.* **194,** 3542–3548 (2015).
955 23. Stevens, B. *et al.* The classical complement cascade mediates CNS
956   synapse elimination. *Cell* **131,** 1164–1178 (2007).
957 24. Gorelik, A. *et al.* Developmental activities of the complement pathway in
958   migrating neurons. *Nature Communications* **8,** 15096 (2017).
959 25. Hong, S. *et al.* Complement and microglia mediate early synapse loss in
960   Alzheimer mouse models. *Science* **352,** 712–716 (2016).
961 26. Vasek, M. J. *et al.* A complement–microglial axis drives synapse loss
962   during virus-induced memory impairment. *Nature* **534,** 538–543 (2016).
963 27. Litvinchuk, A. *et al.* Complement C3aR Inactivation Attenuates Tau
964   Pathology and Reverses an Immune Network Deregulated in Tauopathy
965   Models and Alzheimer's Disease. *Neuron* **100,** 1337–1353.e5 (2018).
966 28. Kempermann, G., Krebs, J. & Fabel, K. The contribution of failing adult
967   hippocampal neurogenesis to psychiatric disorders. *Curr Opin Psychiatry*
968   **21,** 290–295 (2008).
969 29. Cho, K.-O. *et al.* Aberrant hippocampal neurogenesis contributes to
970   epilepsy and associated cognitive decline. *Nature Communications* **6,**
971   6606 (2015).
972 30. Das, T., Ivleva, E. I., Wagner, A. D., Stark, C. E. L. & Tamminga, C. A.
973   Loss of pattern separation performance in schizophrenia suggests
974   dentate gyrus dysfunction. *Schizophrenia Research* **159,** 193–197
975   (2014).
976 31. Gandy, K. *et al.* Pattern Separation: A Potential Marker of Impaired
977   Hippocampal Adult Neurogenesis in Major Depressive Disorder. *Frontiers*
978   *in Neuroscience* **11,** (2017).

979   32.   Dohm-Hansen, S. & Johansson, M. Mnemonic discrimination of object
980   and context is differentially associated with mental health. *Neurobiology*
981   *of Learning and Memory* **173,** 107268 (2020).
982   33.   Sekar, A. *et al.* Schizophrenia risk from complex variation of complement
983   component 4. *Nature* 1–17 (2016). doi:10.1038/nature16549
984   34.   Harold, D. *et al.* Genome-wide association study identifies variants at
985   CLU and PICALM associated with Alzheimer's disease. *Nature Genetics*
986   **41,** 1088–1093 (2009).
987   35.   Rahpeymai, Y. *et al.* Complement: a novel factor in basal and ischemia-
988   induced neurogenesis. *EMBO J* **25,** 1364–1374 (2006).
989   36.   Moriyama, M. *et al.* Complement Receptor 2 Is Expressed in Neural
990   Progenitor Cells and Regulates Adult Hippocampal Neurogenesis.
991   *Journal of Neuroscience* **31,** 3981–3989 (2011).
992   37.   Shi, Q. *et al.* Complement C3-Deficient Mice Fail to Display Age-Related
993   Hippocampal Decline. *Journal of Neuroscience* **35,** 13029–13042 (2015).
994   38.   Perez-Alcazar, M. *et al.* Altered cognitive performance and synaptic
995   function in the hippocampus of mice lacking C3. *Experimental Neurology*
996   **253,** 154–164 (2013).
997   39.   Lian, H., Li, Y., Lu, H.-C. & Zheng, H. NFκB-Activated Astroglial Release
998   of Complement C3 Compromises Neuronal Morphology and Function
999   Associated with Alzheimer's Disease. **85,** 101–115 (2015).
1000   40.   Lledo, P.-M., Alonso, M. & Grubb, M. S. Adult neurogenesis and
1001   functional plasticity in neuronal circuits. *Nat Rev Neurosci* **7,** 179–193
1002   (2006).
1003   41.   Stephan, A. H., Barres, B. A. & Stevens, B. The complement system: an
1004   unexpected role in synaptic pruning during development and disease.
1005   *Annu. Rev. Neurosci.* **35,** 369–389 (2012).
1006   42.   Peterson, S. L., Nguyen, H. X., Mendez, O. A. & Anderson, A. J.
1007   Complement protein C1q modulates neurite outgrowth in vitro and spinal
1008   cord axon regeneration in vivo. *J. Neurosci.* **35,** 4332–4349 (2015).
1009   43.   Shinjyo, N., Ståhlberg, A., Dragunow, M., Pekny, M. & Pekna, M.
1010   Complement-derived anaphylatoxin C3a regulates in vitro differentiation
1011   and migration of neural progenitor cells. *Stem Cells* **27,** 2824–2832
1012   (2009).
1013   44.   Creer, D. J., Romberg, C., Saksida, L. M., van Praag, H. & Bussey, T. J.
1014   Running enhances spatial pattern separation in mice. *Proc. Natl. Acad.*
1015   *Sci. U.S.A.* **107,** 2367–2372 (2010).
1016   45.   Paxinos, G. & Franklin, K. *Paxinos and Franklin's the mouse brain in*
1017   *stereotaxic coordinates*. (2019).
1018   46.   Longair, M. H., Baker, D. A., Bioinformatics, J. A.2011. Simple Neurite
1019   Tracer: open source software for reconstruction, visualization and
1020   analysis of neuronal processes. *Bioinformatics* **27,** 2453-2454 (2011).
1021   47.   Garcia-Segura, L. M. & Perez-Marquez, J. A new mathematical function
1022   to evaluate neuronal morphology using the Sholl analysis. *J. Neurosci.*
1023   *Methods* **226,** 103–109 (2014).
1024   48.   Hvoslef-Eide, M. *et al.* The touchscreen operant platform for testing
1025   working memory and pattern separation in rats and mice. *Nat Protoc* **8,**
1026   2006–2021 (2013).

1027	49.	McTighe, S. M., Mar, A. C., Romberg, C., Bussey, T. J. & Saksida, L. M.
1028		A new touchscreen test of pattern separation: effect of hippocampal
1029		lesions. *Neuroreport* **20,** 881–885 (2009).
1030	50.	Oomen. *et al.* The touchscreen operant platform for testing working
1031		memory and pattern separation in rats and mice. *Nat Protoc* **8,** 2006–
1032		2021 (2013).
1033	51.	Horner, A. E. *et al.* The touchscreen operant platform for testing learning
1034		and memory in rats and mice. *Nat Protoc* **8,** 1961–1984 (2013).
1035	52.	Wright, S. P. Adjusted P-Values for Simultaneous Inference. *Biometrics*
1036		**48,** 1005 (1992).
1037	53.	Llorens-Martín, M., Rábano, A. & Ávila, J. The Ever-Changing
1038		Morphology of Hippocampal Granule Neurons in Physiology and
1039		Pathology. *Frontiers in Neuroscience* **9,** 4217–20 (2016).
1040	54.	Zhao, C. Distinct Morphological Stages of Dentate Granule Neuron
1041		Maturation in the Adult Mouse Hippocampus. *Journal of Neuroscience*
1042		**26,** 3–11 (2006).
1043	55.	Rahimi, O. & Claiborne, B. J. in *The Dentate Gyrus: A Comprehensive*
1044		*Guide to Structure, Function, and Clinical Implications* **163,** 167–181
1045		(Elsevier, 2007).
1046	56.	Bussey, T. J. *et al.* The touchscreen cognitive testing method for rodents:
1047		How to get the best out of your rat. *Learn. Mem.* **15,** 516–523 (2008).
1048	57.	Bogestål, Y. R. *et al.* Signaling through C5aR is not involved in basal
1049		neurogenesis. *J. Neurosci. Res.* **85,** 2892–2897 (2007).
1050	58.	Buss, R. R., Sun, W. & Oppenheim, R. W. Adaptive roles of programmed
1051		cell death during nervous system development. *Annu. Rev. Neurosci.* **29,**
1052		1–35 (2006).
1053	59.	Salter, E. W. *et al.* Complement C3-dependent glutamatergic synapse
1054		elimination in the developing hippocampus is region- and synapse-
1055		specific. *Preprint on BioRxiv* https://doi.org/10.1101/2020.05.20.106930
1056	60.	Cero, C. *et al.* The TLQP-21 peptide activates the G-protein-coupled
1057		receptor C3aR1 via a folding-upon-binding mechanism. *Structure* **22,**
1058		1744–1753 (2014).
1059	61.	Hannedouche, S. *et al.* Identification of the C3a Receptor (C3AR1) as the
1060		Target of the VGF-derived Peptide TLQP-21 in Rodent Cells. *Journal of*
1061		*Biological Chemistry* **288,** 27434–27443 (2013).
1062	62.	Snyder, J. S., Ferrante, S. C. & Cameron, H. A. Late Maturation of Adult-
1063		Born Neurons in the Temporal Dentate Gyrus. *PLoS ONE* **7,** e48757–8
1064		(2012).
1065	63.	Rahimi, O. & Claiborne, B. J. Morphological development and maturation
1066		of granule neuron dendrites in the rat dentate gyrus. *Prog. Brain Res.*
1067		**163,** 167–181 (2007).
1068	64.	Scharfman, H. E., Sollas, A. L., Smith, K. L., Jackson, M. B. & Goodman,
1069		J. H. Structural and functional asymmetry in the normal and epileptic rat
1070		dentate gyrus. *Journal of Comparative Neurology* **454,** 424–439 (2002).
1071	65.	Chawla, M. K. *et al.* Sparse, environmentally selective expression of Arc
1072		RNA in the upper blade of the rodent fascia dentata by brief spatial
1073		experience. *Hippocampus* **15,** 579–586 (2005).
1074	66.	Ramírez-Amaya, V. *et al.* Spatial exploration-induced Arc mRNA and
1075		protein expression: evidence for selective, network-specific reactivation.
1076		*J. Neurosci.* **25,** 1761–1768 (2005).

1077 67. Sahay, A. *et al.* Increasing adult hippocampal neurogenesis is sufficient
1078 to improve pattern separation. *Nature* **472,** 466–470 (2011).
1079 68. Tronel, S. *et al.* Adult-born neurons are necessary for extended
1080 contextual discrimination. *Hippocampus* **22,** 292–298 (2010).
1081 69. Cameron, H. A. & Glover, L. R. Adult neurogenesis: beyond learning and
1082 memory. *Annu Rev Psychol* **66,** 53–81 (2015).
1083 70. Groves, J. O. *et al.* Ablating adult neurogenesis in the rat has no effect on
1084 spatial processing: evidence from a novel pharmacogenetic model. *PLoS*
1085 *Genet* **9,** e1003718 (2013).
1086 71. Saxe, M. D. *et al.* Paradoxical influence of hippocampal neurogenesis on
1087 working memory. *Proc. Natl. Acad. Sci. U.S.A.* **104,** 4642–4646 (2007).
1088 72. Tronel, S. *et al.* Spatial learning sculpts the dendritic arbor of adult-born
1089 hippocampal neurons. *Proc. Natl. Acad. Sci. U.S.A.* **107,** 7963–7968
1090 (2010).
1091 73. Nakashiba, T. *et al.* Young Dentate Granule Cells Mediate Pattern
1092 Separation, whereas Old Granule Cells Facilitate Pattern Completion.
1093 *Cell* **149,** 188–201 (2012).
1094 74. Webler, R. D., Fulton, S., Perera, T. D. & Coplan, J. D. Maturational
1095 phase of hippocampal neurogenesis and cognitive flexibility.
1096 *Neuroscience Letters* **711,** 134414 (2019).
1097 75. Lian, H. *et al.* NFκB-Activated Astroglial Release of Complement C3
1098 Compromises Neuronal Morphology and Function Associated with
1099 Alzheimer's Disease. **85,** 101–115 (2015).
1100 76. Stokowska, A. *et al.* Complement peptide C3a stimulates neural plasticity
1101 after experimental brain ischaemia. *academic.oup.com*
1102 doi:10.1093/brain/aww314
1103 77. Coulthard, L. G., Hawksworth, O. A., Conroy, J., Lee, J. D. & Woodruff, T.
1104 M. Complement C3a receptor modulates embryonic neural progenitor cell
1105 proliferation and cognitive performance. *Molecular Immunology* **101,**
1106 176–181 (2018).
1107 78. Pozo-Rodrigálvarez, A., Ollaranta, R., Skoog, J., Pekny, M. & Pekna, M.
1108 Hyperactive Behavior and Altered Brain Morphology in Adult Complement
1109 C3a Receptor Deficient Mice. *Front. Immunol.* **12,** 604812 (2021).
1110 79. Schafer, D. P. *et al.* Microglia sculpt postnatal neural circuits in an activity
1111 and complement-dependent manner. *Neuron* **74,** 691–705 (2012).
1112 80. Scharfman, H. E. & Hen, R. NEUROSCIENCE: Is More Neurogenesis
1113 Always Better? *Science* **315,** 336–338 (2007).
1114 81. Mahmoud, R., Wainwright, S. R. & Galea, L. A. M. Sex hormones and
1115 adult hippocampal neurogenesis: Regulation, implications, and potential
1116 mechanisms. *Frontiers in Neuroendocrinology* **41,** 129–152 (2016).
1117 82. Yagi, S. & Galea, L. A. M. Sex differences in hippocampal cognition and
1118 neurogenesis. *Neuropsychopharmacology* 1–14 (2018).
1119 doi:10.1038/s41386-018-0208-4
1120 83. Hattiangady, B., Rao, M. & Shetty, A. Chronic temporal lobe epilepsy is
1121 associated with severely declined dentate neurogenesis in the adult
1122 hippocampus. *Neurobiol. Dis.* **17,** 473–490 (2004).
1123 84. Aronica, E. *et al.* Complement activation in experimental and human
1124 temporal lobe epilepsy. *Neurobiol. Dis.* **26,** 497–511 (2007).

1125   85.   Jamali, S. *et al.* Large-scale expression study of human mesial temporal
1126   lobe epilepsy: evidence for dysregulation of the neurotransmission and
1127   complement systems in the entorhinal cortex. *Brain* **129,** 625–641 (2006).
1128   86.   DeCarolis, N. A. & Eisch, A. J. Hippocampal neurogenesis as a target for
1129   the treatment of mental illness: A critical evaluation. *Neuropharmacology*
1130   **58,** 884–893 (2010).
1131   87.   Bernard, M. *et al.* Characterization of C3a and C5a receptors in rat
1132   cerebellar granule neurons during maturation. Neuroprotective effect of
1133   C5a against apoptotic cell death. *J. Biol. Chem.* **279**, 43487-43496 (2004).